

GRAPH POTENTIALS AND TOPOLOGICAL QUANTUM FIELD THEORIES

PIETER BELMANS, SERGEY GALKIN, AND SWARNAVA MUKHOPADHYAY

ABSTRACT. We introduce graph potentials, which are Laurent polynomials associated to (colored) trivalent graphs. We show that the birational type of the graph potential only depends on the homotopy type of the colored graph, and use this to define a topological quantum field theory. We end by giving an efficient computational method to compute its partition function. This is the first paper in a series, and we give a survey of the applications of graph potentials in the other parts.

CONTENTS

1. Introduction	1
1.1. Graph potentials	2
1.2. Overview of the results	4
1.3. Applications of graph potentials	6
2. Graph potentials	8
2.1. Definition	9
2.2. Elementary transformations	13
2.3. Periods of Laurent polynomials	18
3. Topological quantum field theories from graph potentials	19
3.1. Restricted TQFT	20
3.2. The graph potential TQFT	21
4. Computing periods via the graph potential TQFT	25
References	36

1. INTRODUCTION

In this paper we introduce *graph potentials*, a collection of Laurent polynomials associated to trivalent graphs, that enjoys remarkable symmetries. Section 1.1 is a general self-contained elementary overview, intended as an invitation for the interested reader to play with variations on the construction.

The main result of this paper is the construction of a novel topological quantum field theory, the *graph potential field theory*. This result encodes the hidden structure/symmetries

of graph potentials, and explains how their invariance properties are related to the geometry of Riemann surfaces, their degenerations and Thurston's cut systems. The partition functions are equal to high-dimensional integrals (the so-called *periods* for a family of level sets), and the graph potential field theory is the first and the only known efficient method for their computation. For more details, see Section 1.2.

This paper is one of recommended entry points to a series of our works on conformal field theory, mirror symmetry, and moduli spaces of rank 2 vector bundles with fixed determinant on algebraic curves of genus $g \geq 2$. The relationship between graph potentials and the geometry of moduli spaces, as well as different aspects of mirror symmetry for these objects, is discussed in Section 1.3, where we describe the big picture for graph potentials and the follow-up works [10, 9].

1.1. Graph potentials. We will first introduce graph potentials in an abstract way, without reference to other topics of interest or applications. It would be interesting to find new choices of the input in the construction. Our choice of input is discussed in (8), and its relevance is proven by the results discussed in Section 1.3.

General construction. Let $Y(a, b, c)$ be a function (defined on some space equipped with a volume form) which is symmetric in its arguments, such that

$$(1) \quad Y(a, b, s) + Y(c, d, s) = Y(a, c, t) + Y(b, d, t) = Y(a, d, u) + Y(b, c, u)$$

for some volume-preserving transformation relating the variables.

Let $\gamma = (V, E)$ be a trivalent graph, possibly with half-edges (or leaves). Let v be a trivalent vertex, whose edges are labelled by a, b, c , as in

$$(2) \quad \begin{array}{c} a \\ | \\ v \\ / \quad \backslash \\ b \quad c \end{array}$$

We define the *vertex potential* W_v as $Y(a, b, c)$. To emphasize the dependence on v we also write a_v, b_v, c_v .

Next, the *graph potential* W_γ is the sum of the vertex potentials associated to the (internal) vertices, i.e.

$$(3) \quad W_\gamma := \sum_{v \in V} W_v$$

where $W_v = W_v(a_v, b_v, c_v)$. This is an expression in $3(g - b_0) + 2n$ arguments, where we let $b_0 = b_0(\gamma)$ denote the number of connected components, $g = b_1(\gamma)$ is the genus of the graph, and n is the number of half-edges. There are $3(g - b_0) + n$ internal variables and n external (or leaf) variables associated to the half-edges.

The functional equation (1) explains how the graph potentials behave under *mutation*. Such a mutation will produce a new trivalent graph with a new graph potential associated to it, and controlling this operation will yield important invariance properties of graph potentials, see Section 2.2. The upshot is that the different W_γ glue to a single function $W_{g,n}$, and the W_γ for different choices of γ are restrictions to different torus charts.

Partition functions from graph potentials. Applying a Fourier-like transform we can write

$$(4) \quad \exp(\mathbf{Y}(a, b, c)) = \sum_{i,j,k} F(i, j, k) a^i b^j c^k$$

for a function $F(i, j, k)$. These functions satisfy the Frobenius equation

$$(5) \quad \sum_m F(i, j, m) F(k, l, -m) = \sum_n F(i, k, n) F(j, l, -n).$$

This equation hints at an important compatibility property, culminating in Theorems [A](#) and [B](#).

We can moreover consider the integration over the internal variables w_1, \dots, w_{3g-3+n} , and define the symmetric function

$$(6) \quad Z_g(z_1, \dots, z_n) := \iiint \exp(W_\gamma(z_1, \dots, z_n; w_1, \dots, w_{3g-3+n}))$$

in the n external variables z_1, \dots, z_n . This function only depends on the genus g of the graph γ , and it satisfies the rules

$$(7) \quad \begin{cases} Z_{g+g'}(z_1, \dots, z_{n+n'}) = \iiint Z_g(z_1, \dots, z_n, w) Z_{g'}(z_{n+1}, \dots, z_{n+n'}, w) \\ Z_{g+1}(z_1, \dots, z_n) = \iiint Z_g(z_1, \dots, z_n, w, w). \end{cases}$$

This type of compatibilities, ultimately governed by (1), allow us to study the partition functions associated to graph potentials.

Our choice of potential. In the remainder of the paper we will focus on a specific choice of the function \mathbf{Y} , namely the Laurent polynomial

$$(8) \quad \mathbf{Y}(a, b, c) = \frac{a}{bc} + \frac{b}{ac} + \frac{c}{ab} + abc.$$

The domain of the function is the torus $(\mathbb{C}^\times)^3$. The transformation that gives a solution to (1) is the rational change of coordinates

$$(9) \quad s \cdot (ab + cd) = t \cdot (ac + bd) = u \cdot (ad + bc).$$

This transformation preserves the logarithmic rational volume forms

$$(10) \quad \omega_a \wedge \omega_b \wedge \omega_c \wedge \omega_* \quad * \in \{s, t, u\}$$

where $\omega_a = d \log a = \frac{da}{a}$ is the Haar measure for the multiplicative group.

We can give an interpretation of this choice, independent of the role it will play for us, as follows. Consider a tetrahedron inscribed in the cube $[0, \frac{D}{2}]^3$, whose facets are bounded by the conditions

$$(11) \quad \begin{cases} A \leq B + C, & B \leq A + C, & C \leq A + B \\ & A + B + C \leq D \end{cases}$$

This tetrahedron can be seen as the moduli space of geodesic triangles on a sphere of radius $R = \frac{D}{2\pi}$. The first inequalities are the classical triangle inequalities, and the last one is a quantum bound of the perimeter.

After the substitution $(a, b, c, d) = (\exp A, \exp B, \exp C, \exp(-D))$ the Laurent polynomial (8) becomes a generating function of the inequalities (11), which is invariant with respect to translations by $2\pi\sqrt{-1}(A, B, C)$ for (A, B, C) satisfying

$$(12) \quad \pm A \pm B \pm C \in \mathbb{Z}.$$

If we let A, B, C be real (resp. complex) numbers, then a, b, c are real positive (resp. complex non-zero), and the Haar measure ω_a in the coordinate a becomes the Lebesgue measure in the coordinate A .

The definition of graph potentials for (8) will, instead of trivalent graphs with half-edges, involves colored trivalent graphs (without half-edges), where we let a trivalent vertex v be either uncolored \circ or colored \bullet . We will explain this in Section 2.1.

It would be interesting to find other functions $Y(a, b, c)$, study their partition functions, and relate them to geometry.

A sneak preview of the geometry to explain our choice of potential. As explained in Section 1.3 we will relate graph potentials to the moduli space $M_C(2, \mathcal{L})$ of rank 2 vector bundles. The first case to consider is for $g = 2$, so let C be a smooth projective curve of genus 2. In this case an explicit description of $M_C(2, \mathcal{L})$ due Newstead and Narasimhan-Ramanan exists [38, 37]: it can be written as

$$(13) \quad M_C(2, \mathcal{L}) \cong Q_1 \cap Q_2 \subset \mathbb{P}^5$$

where Q_1, Q_2 are smooth quadric hypersurfaces determined by C .

These varieties degenerate to a *toric* Fano threefold with six ordinary double points. For the (smooth) intersection of quadrics in \mathbb{P}^5 we have the toric degeneration given by the (singular) intersection of quadrics with equations

$$(14) \quad Z_0 Z_1 = Z_2 Z_3 = Z_4 Z_5.$$

As a toric variety it is described by the polytope which is the convex hull of the vertices $(\pm 1, \pm 1, \pm 1)$. This toric variety has terminal singularities, and its 6 ordinary double points admit a small resolution of singularities.

The graph potential associated to the (colored) trivalent graph of genus $g = 2$

$$(15) \quad \begin{array}{c} x \\ \circ \text{---} \text{---} \bullet \\ y \\ 1 \quad z \quad 2 \end{array}$$

is closely related to the polytope defining the toric degeneration, and takes on the form

$$(16) \quad \tilde{W} = xyz + \frac{x}{yz} + \frac{y}{xz} + \frac{z}{xy} + \frac{1}{xyz} + \frac{yz}{x} + \frac{xz}{y} + \frac{xy}{z}.$$

The classical period of the Laurent polynomial $\tilde{W}: \mathbb{G}_m^3 \rightarrow \mathbb{A}^1$ agrees with the quantum period of $M_C(2, \mathcal{L})$, as computed in [12], and hence the graph potential captures certain symplecto-geometric aspects of $M_C(2, \mathcal{L})$. We will elaborate further on this in Section 1.3.

1.2. Overview of the results. We will now discuss the results proven in this paper, for the choice of potential in (8).

Graph potentials under elementary transformations. The first result we will prove is an invariance property of graph potentials under appropriate changes of the trivalent graph. To motivate this result, recall that one way in which a trivalent graph of genus g arises is as a degeneration of a smooth projective curve C of genus g into a nodal curve with only rational components. Such a curve is also called a graph curve in Bayer–Eisenbud [6], and its dual graph gives γ . Alternatively, such trivalent graphs can be seen as pair of pants decompositions of C , considered as a Riemann surface.

Different degenerations, and different pair of pants decompositions are related to each other by elementary transformations à la Hatcher–Thurston, which act on the trivalent graph. We prove that graph potentials are suitably invariant under these elementary transformations:

Theorem A. *Let (γ, c) and (γ', c') be two trivalent colored graphs related by elementary transformations. Then the graph potentials $\widetilde{W}_{\gamma, c}$ and $\widetilde{W}_{\gamma', c'}$ are identified via a rational change of coordinates.*

The proof of this theorem is given in Section 2.2, and it expresses the invariance of graph potentials under mutations. In [10] we will further discuss the link between the mutations in Theorem A, and the mutation of potentials in the context of mirror symmetry.

Associated to a Laurent polynomial we have its classical period. The relevance of this invariant is discussed in Section 1.3. The invariance properties of graph potentials from Theorem A allow us to show in Corollary 2.18 that classical periods of graph potentials *only depend* on the number of vertices and the parity of the coloring.

The graph potential topological quantum field theory. Inspired by this invariance under elementary transformations, we will define in Construction 3.10 a topological quantum field theory, and call it the *graph potential field theory*. In other words, we have found a new solution to the Witten–Dijkgraaf–Verlinde–Verlinde (WDVV) equation.

Its partition function $Z^{\text{sp}}(t)$ (for any $t \in \mathbb{R}$) assigns to the pair of pants $\Sigma_{0,3}$ with $1 + \epsilon$ anticlockwise oriented circles, for $\epsilon \in \{0, 1\}$, the appropriately colored vertex potential, i.e.

$$(17) \quad Z^{\text{sp}}(t)(\Sigma_{0,3}) := \exp\left(t\widetilde{W}_{v,\epsilon}(x, y, z)\right) \in \ell^2(\mathbb{Z})^{\otimes 3}.$$

Here $\ell^2(\mathbb{Z})$ is the Hilbert space of square-integrable real series indexed by \mathbb{Z} . A countable orthonormal basis is given by $\{x^i\}_{i \in \mathbb{Z}}$ and any element of $\ell^2(\mathbb{Z})$ can be written as $\sum_{i \in \mathbb{Z}} a_i x^i$ such that $\sum_{i \in \mathbb{Z}} a_i^2 < \infty$. Because the potential takes values in an infinite-dimensional Hilbert space, we will need to restrict the bordism category suitably.

The properties of the graph potential can then be used to show the following theorem.

Theorem B. *Let $t \in \mathbb{R}$. The graph potential field theory $Z^{\text{sp}}(t)$ is a two-dimensional topological quantum field theory on a suitably restricted bordism category, with values in Hilbert spaces.*

Observe that our TQFT takes values in $\ell^2(\mathbb{Z})$, and that it is not related to the usual $(1+1)$ -TQFT coming from the fusion ring of conformal blocks.

The existence of this TQFT shows why it is a powerful idea to consider moduli spaces of vector bundles on curves *for all genera simultaneously* when one is interested in mirror

symmetry aspects of these Fano varieties. In a different direction, González-Prieto–Logares–Muñoz have constructed a topological quantum field theory computing Hodge–Deligne polynomials for representation varieties [22].

The topological quantum field theory in Theorem B gives a powerful computational tool to compute classical periods of graph potentials. This is discussed in Section 4.

There is in fact an abundance of various flavours of field theories, in this series of papers, and the works we build upon. Indeed, in this work we have introduced a novel *topological quantum field theory* to compute periods of graph potentials. The results we build upon in [10] to construct and study toric degenerations use the *conformal field theory* given by conformal blocks [7, 43, 42]. On the other hand, the study of classical and quantum periods in [10] features both *cohomological field theories* and *symplectic field theories* (see [28] and [1, 11, 17]).

Furthermore, the cohomological and symplectic field theories in turn can be compared using a *tropical field theory*, which can be seen as an intermediary between them [33, 34, 32, 30, 31]. Finally, at the end of this introduction we speculate on the relationship between our work and the construction of the (still conjectural) 4-dimensional *Donaldson–Floer quantum field theory*.

1.3. Applications of graph potentials. As this is the first paper in a series we will now outline the results in the next installments.

Whilst they do not play a role in the current paper, our original motivation to introduce graph potentials was to study the algebro- and symplecto-geometric aspects of the moduli space $M_C(2, \mathcal{L})$ of rank 2 vector bundles with fixed determinant on a smooth projective curve C . The mirror dual of $M_C(2, \mathcal{L})$ is expected to be a cluster-like variety equipped with a regular function, the so-called Landau–Ginzburg potential (closely related to the Floer potential). We propose in [10, 9] that graph potentials can be seen as (building blocks of) mirrors to $M_C(2, \mathcal{L})$.

Enumerative mirror symmetry. In [10] we will discuss aspects of the symplectic geometry of $M_C(2, \mathcal{L})$, and relate it to the algebraic geometry of graph potentials.

In particular we will consider the *quantum period* $G_{M_C(2, \mathcal{L})}(t)$, a generating function for closed genus zero Gromov–Witten invariants with descendants and primary field being a point, which can be also defined using the operator of quantum multiplication by the first Chern class, whose coefficients are closed genus zero correlators without descendants but with two arbitrary cohomology insertions.

The invariant associated to graph potentials is the *classical period*, the constant terms of powers of the Laurent polynomial. The agreement of these two sequences of numbers is an important litmus test for mirror symmetry of Fano varieties, and forms the main result of [10].

Homological mirror symmetry. In [9] we will discuss certain decompositions that arise in the study of $M_C(2, \mathcal{L})$ and graph potentials. Since $M_C(2, \mathcal{L})$ is a Fano manifold, its bounded derived category of coherent sheaves is expected to have a homological mirror dual partner in the sense of Kontsevich’s homological mirror symmetry conjecture, cf. [26] for Calabi–Yau varieties and [27, page 30] for the Fano version.

This mirror dual partner is expected to be a pair (Y, f) , where Y is a smooth quasiprojective variety and f a regular function on it. The Laurent polynomials discussed before are then restrictions of the Landau–Ginzburg potential f to a torus $\mathbb{G}_m^n \subseteq Y$. For more information on these pairs, and their “tamings” one is referred to [25].

Assuming that the categories of symplectic origin, namely the so-called Fukaya category of (graded) immersed (e.g. embedded) coisotropic (e.g. Lagrangian) subvarieties in $M_C(2, \mathcal{L})$ decorated with a flat unitary connection and the analogous Fukaya–Seidel category of vanishing Lagrangian thimbles in Y , are well-defined, the spaces $M_C(2, \mathcal{L})$ and (Y, f) are called *homologically mirror dual* if

- the derived category of coherent sheaves on $M_C(2, \mathcal{L})$ is equivalent to the derived Fukaya–Seidel category of (Y, f) ,
- the derived Fukaya category of $M_C(2, \mathcal{L})$ is equivalent to the matrix factorization category of (Y, f) .

We also refer the reader to [24, Conjecture 2.3] for a general discussion on Landau–Ginzburg models and homological mirror symmetry conjectures.

A natural approach to tackle the first equivalence starts with finding *semiorthogonal decompositions* on either side of the mirror. We propose in [9, Conjecture A] a conjectural semiorthogonal decomposition for $\mathbf{D}^b(M_C(2, \mathcal{L}))$, independently suggested by Narasimhan. For a description of the state-of-the-art we refer to op. cit. As evidence for this conjecture we provide in [9, Theorem C] a *motivic decomposition* of $M_C(2, \mathcal{L})$ (resp. $\mathbf{D}^b(M_C(2, \mathcal{L}))$) in the Grothendieck rings of varieties and categories.

With respect to the graph potentials introduced in this paper, it becomes interesting to study the second equivalence of categories. Here one aims to find *orthogonal decompositions* on either side of the mirror. For the derived Fukaya category there is a natural decomposition in terms of eigenvalues of the quantum multiplication, which is described by Muñoz [35, 36]. In [9, Theorem B] we show that this eigenvalue decomposition is mirrored by a critical value decomposition of graph potentials. This in turns gives further evidence for the conjectured semiorthogonal decomposition.

Reconstruction results. In [8] we discuss how the Newton polytope of the graph potential determines the graph and its coloring. This is a reconstruction result which on the algebro-geometric side mirror to graph potentials corresponds to a *combinatorial non-abelian Torelli theorem*. We refer to op. cit. for more context and applications.

Outlook: mirror approach to the Atiyah–Floer conjecture. To end the introduction, we speculate on a variation on the theme of the Atiyah–Floer conjecture, suggested by mirror symmetry, and how graph potentials could lead to progress.

The Atiyah–Floer conjecture from [4] states that two homology theories, both introduced by Floer, are isomorphic. One is the instanton Floer homology $\mathrm{HF}^{\mathrm{inst}}(B)$ of a 3-manifold B [18]. The other is the symplectic Floer homology of two Lagrangian subvarieties $R(B_-)$ and $R(B_+)$ inside a symplectic variety $R(\Sigma)$ associated to a Heegaard splitting $B = B_- \cup_{\Sigma} B_+$ into two handlebodies along a common boundary surface Σ [19]. The notation $R(*)$ stands for the moduli space of flat $\mathrm{SU}(2)$ -connections on $* = \Sigma, B_{\pm}, B$. The (smooth locus of the) variety $R(\Sigma)$ is equipped with the Narasimhan–Atiyah–Bott–Goldman symplectic structure, for which $R(B_{\pm}) \rightarrow R(\Sigma)$ are Lagrangian embeddings.

Donaldson proposed to extend and categorify the Atiyah–Floer conjecture. For an overview one is referred to [13]. Associated to the surface Σ one then has a category $\mathcal{C}(\Sigma)$, whilst the handlebodies B_{\pm} with boundary $\partial B_{\pm} = \Sigma$ define objects in $\mathcal{C}(\Sigma)$. This assignment is subject to the condition that the morphism spaces are identified with the symplectic Floer homology. This (provisional) extended 4-dimensional TQFT is known as *Donaldson–Floer theory*. The category $\mathcal{C}(\Sigma)$ should be a Fukaya-like category for the symplectic variety $R(\Sigma)$, whereas the Lagrangian subvarieties $R(B_{\pm})$ define objects in it.

On the other side of the mirror we have graph potentials (and more complicated Landau–Ginzburg models constructed using graph potentials), and their categories of matrix factorizations. Similar to how categories of matrix factorizations of the potential x^n appear as basic building blocks of Khovanov–Rozansky field theories, the categories of matrix factorizations of graph potentials are expected to be mirror dual to the Fukaya categories of the symplectic varieties $R(\Sigma)$.

The upshot of this approach is that it is purely algebraic, whereas on the symplectic side one needs to do complicated analysis. Likewise, $R(\Sigma)$ is singular, complicating the study of the Fukaya category even further. In particular, our work suggests how one could try to construct Donaldson–Floer theory on the other side of the mirror.

Acknowledgments. We want to thank Catharina Stroppel for interesting discussions.

This collaboration started in Bonn in January–March 2018 during the second author’s visit to the “Periods in Number Theory, Algebraic Geometry and Physics” Trimester Program of the Hausdorff Center for Mathematics (HIM) and the first and third author’s stay in the Max Planck Institute for Mathematics (MPIM), and the remaining work was done in the Tata Institute for Fundamental Research (TIFR) during the second author’s visit in December 2019–March 2020 and the first author’s visit in February 2020. We would like to thank HIM, MPIM and TIFR for the very pleasant working conditions.

Several computations and experiments were performed using Pari/GP [41].

The first author was partially supported by the FWO (Research Foundation–Flanders). The third author was partially supported by the Department of Atomic Energy, India, under project no. 12-R&D-TFR-5.01-0500 and also by the Science and Engineering Research Board, India (SRG/2019/000513).

2. GRAPH POTENTIALS

We will consider trivalent graphs of genus g . Such graphs are associated to pair of pants decompositions of compact orientable surfaces in the sense of Hatcher–Thurston [23]. These are collections of disjoint circles on a surface Σ such that their complement is the disjoint union of spheres with 3 holes, also known as “pairs of pants” or trinions. In this section we associate a Laurent polynomial to each trivalent graph, and study how different Laurent polynomials associated to different graphs are related to each other.

The dual of the pair of pants can be encoded as follows:

$$(18) \quad \begin{array}{c} \text{---} \\ \text{---} \\ \text{---} \end{array} = \begin{array}{c} \text{---} \\ \text{---} \\ \text{---} \end{array}$$

and to a decomposition of Σ into such pairs of pants we associate the graph whose vertices are the pairs of pants, and whose edges indicate how the pairs of pants are glued together.

Loops arise from cutting a genus 1 surface with 1 puncture by a circle. For every pants decomposition one thus obtains a trivalent graph.

For now we will consider trivalent graphs without making this link to geometry and topology explicit, but this will be important later.

2.1. Definition. Let $\gamma = (V, E)$ be an undirected trivalent graph (possibly containing loops), which we will assume to be connected, and whose first Betti number is g . Hence

$$(19) \quad \begin{aligned} \#V &= 2g - 2, \\ \#E &= 3g - 3. \end{aligned}$$

Recall that the homology (resp. cohomology) of a graph with coefficients in a ring R (which for us will be either \mathbb{Z} or \mathbb{F}_2) takes $C_0(\gamma, R) = R^V$ and $C_1(\gamma, R) = R^E$ with differential given by the incidence matrix after choosing an orientation of the graph (resp. the R -linear dual of the incidence matrix). Hence $\text{rk } H_0(\gamma, R)$ is the number of connected components, and $\text{rk } H_1(\gamma, R)$ is the genus of the graph. Because we only consider the differential when $R = \mathbb{F}_2$ the choice of orientation is irrelevant for us.

We will denote

$$(20) \quad \tilde{N}_\gamma := C^1(\gamma, \mathbb{Z})$$

the free abelian group of 1-cochains on γ , and

$$(21) \quad \tilde{M}_\gamma := C_1(\gamma, \mathbb{Z})$$

the free abelian group of 1-chains.

Let $v \in V$ be a vertex. It is adjacent to the edges $e_{v_i}, e_{v_j}, e_{v_k} \in E$ (which might coincide if there is a loop). We will denote the sublattice of \tilde{N}_γ generated by the cochains x_i, x_j, x_k for which $x_i(e_{v_a}) = \delta_{i,v_a}$ by \tilde{N}_v .

Inside \tilde{N}_v we consider the sublattice N_v generated by the eight cochains $\{\pm x_i \pm x_j \pm x_k\}$. Using these we define the sublattice

$$(22) \quad N_\gamma \subseteq \tilde{N}_\gamma$$

as the image of the natural morphism $\bigoplus_{v \in V} N_v \rightarrow \tilde{N}_\gamma$.

We have the associated tori $T_\gamma^\vee := \text{Spec } \mathbb{C}[N_\gamma]$ and $\tilde{T}_\gamma^\vee := \text{Spec } \mathbb{C}[\tilde{N}_\gamma]$, so that N_γ and \tilde{N}_γ are realized as the character lattice of T_γ^\vee and \tilde{T}_γ^\vee respectively, and hence as the cocharacter lattices of T_γ and \tilde{T}_γ .

The inclusion (22) induces an isogeny of the tori $\tilde{T}_\gamma^\vee \rightarrow T_\gamma^\vee$, whose kernel

$$(23) \quad A_\gamma := \text{Hom}(\tilde{N}_\gamma/N_\gamma, \mathbb{C}^\times) = (\tilde{N}_\gamma/N_\gamma)^\vee,$$

(which is isomorphic to $\mathbb{F}_2^{\oplus g}$) we wish to describe explicitly.

Consider the dual lattices $M_\gamma := N_\gamma^\vee$ and $\tilde{M}_\gamma := \tilde{N}_\gamma^\vee$, for which we have $\tilde{M}_\gamma \subseteq M_\gamma$, and $A_\gamma \cong M_\gamma/\tilde{M}_\gamma$. The following lemma summarizes the situation.

Lemma 2.1. *We have that*

$$(24) \quad \begin{aligned} M_Y &= \left\{ m = \sum_{e \in E} w_e e \mid w_e \in \mathbb{R}, \forall n \in N_Y : \langle n, m \rangle \in \mathbb{Z} \right\} \\ &= \left\{ m = \sum_{e \in E} w_e e \mid w_e \in \frac{1}{2}\mathbb{Z}, \forall v \in V : w_{e_i} + w_{e_j} + w_{e_k} \in \mathbb{Z} \right\} \end{aligned}$$

and

$$(25) \quad A_Y \cong H_1(\gamma, \mathbb{F}_2).$$

Here e_i, e_j, e_k are edges adjacent to the vertex v .

In particular we also see that rational functions on the torus T_Y are A_Y -invariant functions on the torus \tilde{T}_Y .

Colorings. Next we introduce colorings. We will use these to conveniently deal with a generalization of the class of trivalent graphs, where half-edges are allowed. Using colorings we can reduce such situations (which will correspond to punctured surfaces) in the cases that we are interested in to the already considered case of trivalent graphs without half-edges.

Definition 2.2. Let $\gamma = (V, E)$ be a trivalent graph. A *coloring* is a function $c: V \rightarrow \mathbb{F}_2$, interpreted as an \mathbb{F}_2 -valued 0-chain on γ .

If $c(v) = 0$ we say that v is *uncolored*, and if $c(v) = 1$ we say that v is *colored*. When drawing a graph, uncolored corresponds to a circle \circ whilst colored corresponds to a disk \bullet . If it can be either we will indicate this by drawing \ominus .

We can now introduce one of the main objects of this paper. In Section 4 we will generalize this definition to also include half-edges, but for now this definition suffices.

Definition 2.3. Let $\gamma = (V, E)$ be a trivalent graph, and let $c: V \rightarrow \mathbb{F}_2$ be a coloring. Let e_1, \dots, e_{3g-3} be an enumeration of the edges. We will denote x_i the coordinate variable in $\mathbb{Z}[\tilde{N}_\gamma]$ associated to e_i .

Let $v \in V$ be a vertex, and denote e_i, e_j, e_k the three edges incident to it. Then the *vertex potential* is the Laurent polynomial

$$(26) \quad \tilde{W}_{v,c} := \sum_{\substack{(s_i, s_j, s_k) \in \mathbb{F}_2^{\otimes 3} \\ s_i + s_j + s_k = c(v)}} x_i^{(-1)^{s_i}} x_j^{(-1)^{s_j}} x_k^{(-1)^{s_k}}$$

in $\mathbb{Z}[\tilde{N}_v]$. Observe that $\tilde{W}_{v,c}$ is in the image of $\mathbb{Z}[N_v]$ in $\mathbb{Z}[\tilde{N}_v]$.

Then we define the *graph potential* as the Laurent polynomial

$$(27) \quad \tilde{W}_{Y,c} := \sum_{v \in V} \tilde{W}_{v,c}$$

in $\mathbb{Z}[\tilde{N}_Y]$. Similarly $\tilde{W}_{Y,c}$ is in the image of $\mathbb{Z}[N_Y]$ in $\mathbb{Z}[\tilde{N}_Y]$. If c is the zero 0-chain, we will write $\tilde{W}_{v,0}$ and $\tilde{W}_{Y,0}$.

By construction we have the following result.

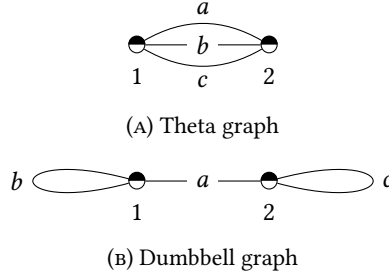


FIGURE 1. Trivalent genus 2 graphs

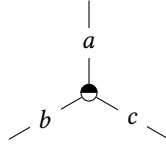
Lemma 2.4. *The graph potential $\widetilde{W}_{Y,c}$ descends to a regular function $W_{Y,c}$ on the torus T_Y^\vee (respectively the toric variety \widetilde{T}_Y^\vee) of the toric variety of $X_{P_{Y,c},M_Y}$ (respectively $X_{P_{Y,c},\widetilde{M}_Y}$).*

In other words, we have a commutative diagram

$$(28) \quad \begin{array}{ccc} \widetilde{T}_Y^\vee & & \\ \downarrow & \searrow \widetilde{W}_{Y,c} & \\ T_Y^\vee & \xrightarrow{W_{Y,c}} & \mathbb{A}^1 \end{array}$$

We will now make the constructions explicit.

Example 2.5. We consider the following local picture of a trivalent vertex.



Then the vertex potentials are precisely

$$(29) \quad \begin{aligned} \widetilde{W}_{Y,0} &= abc + \frac{a}{bc} + \frac{b}{ac} + \frac{c}{ab}, \\ \widetilde{W}_{Y,1} &= \frac{1}{abc} + \frac{ab}{c} + \frac{ac}{b} + \frac{bc}{a}. \end{aligned}$$

There are two trivalent graphs with 2 vertices, which we will call the Theta graph and dumbbell graph respectively, and they are given in Figures 1(a) and 1(b).

Example 2.6 (Theta graph). We consider the Theta graph, labeled as in Figure 1(a). It is a trivalent graph of genus 2. We will consider two colorings for this graph, which will suffice for us by Corollary 2.9. Let c denote the non-trivial coloring given by $c(1) = 0$, $c(2) = 1$. Then we have

$$(30) \quad \widetilde{W}_{Y,0} = 2 \left(abc + \frac{a}{bc} + \frac{b}{ac} + \frac{c}{ab} \right),$$

$$(31) \quad \widetilde{W}_{Y,c} = abc + \frac{a}{bc} + \frac{b}{ac} + \frac{c}{ab} + \frac{1}{abc} + \frac{bc}{a} + \frac{ac}{b} + \frac{ab}{c}.$$

Example 2.7 (Dumbbell graph). Alternatively for $g = 2$ we can consider the dumbbell graph, labeled as in Figure 1(b). We will consider two colorings for this graph, which will suffice for us by Corollary 2.9. Let c denote the non-trivial coloring given by $c(1) = 0$, $c(2) = 1$. Then we have

$$(32) \quad \widetilde{W}_{\gamma,0} = ab^2 + \frac{a}{b^2} + \frac{4}{a} + ac^2 + \frac{a}{c^2},$$

$$(33) \quad \widetilde{W}_{\gamma,c} = ab^2 + \frac{a}{b^2} + \frac{2}{a} + \frac{1}{ac^2} + 2a + \frac{c^2}{a}.$$

Independence of coloring for graph potentials. The graph potential depends a priori on the graph γ and the coloring $c \in C_0(\gamma, \mathbb{F}_2)$. But in fact we can identify many graph potentials as follows.

If $e \in E$ is an edge connecting the vertices v and v' of the graph, then we have an associated 1-chain $[e] \in C_1(\gamma, \mathbb{F}_2)$. Its boundary is $\partial[e] = [v] + [v'] \in C_0(\gamma, \mathbb{F}_2)$. This allows us to modify colorings c by flipping the color of v and v' , preserving the parity of the coloring. Its effect on the graph potential is explained by the following lemma.

Lemma 2.8. *Let (γ, c) be a graph together with a coloring c . Let $\{x_i\}$ be a system of coordinates associated to γ . Let e_k be an edge, and set $c' := c + \partial[e_k]$. Then we have the equality of graph potentials*

$$(34) \quad \widetilde{W}_{\gamma,c} = \widetilde{W}_{\gamma,c'}$$

after the biregular automorphism

$$(35) \quad x_i \mapsto \begin{cases} x_i & i \neq k \\ x_i^{-1} & i = k \end{cases}$$

of the algebraic torus $\text{Spec } \mathbb{Z}[x_1^\pm, \dots, x_{3g-3}^\pm]$. Moreover we get a biregular automorphism of T_γ^\vee that identifies $W_{\gamma,c}$ and $W_{\gamma,c'}$.

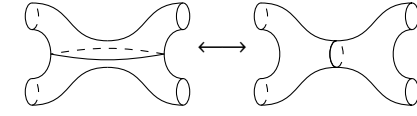
Proof. We only need to consider v and v' , as the vertex potentials for the other vertices are not modified. It also suffices to consider v . The vertex potentials are

$$(36) \quad \begin{aligned} \widetilde{W}_{v,c} &= \sum_{\substack{(s_i, s_j, s_k) \in \mathbb{F}_2^{\oplus 3} \\ s_i + s_j + s_k = c(v)}} x_i^{(-1)^{s_i}} x_j^{(-1)^{s_j}} x_k^{(-1)^{s_k}} \\ \widetilde{W}_{v,c'} &= \sum_{\substack{(s_i, s_j, s_k) \in \mathbb{F}_2^{\oplus 3} \\ s_i + s_j + s_k = c(v)+1}} x_i^{(-1)^{s_i}} x_j^{(-1)^{s_j}} x_k^{(-1)^{s_k}} \end{aligned}$$

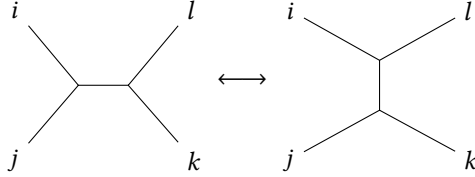
and these sums agree after the given biregular automorphisms. More precisely, we partition $\mathbb{F}_2^{\oplus 3}$ as $\{(0, 0, 0), (0, 1, 1), (1, 0, 1), (1, 1, 0)\} \sqcup \{(0, 0, 1), (0, 1, 0), (1, 0, 0), (1, 1, 1)\}$ and the given biregular automorphism exchanges these subsets, but then the vertex potentials are precisely identified using the given biregular automorphism.

The second part of the proposition follows directly from the fact that each element of A_γ is of order two and it acts on the variables x_i 's by a character and the biregular automorphism (36) either fixes the variables or inverts them. \square

Because $C_1(\gamma, \mathbb{F}_2)$ is generated by the 1-chains $[e_k]$ where e_k runs over the edges, we obtain the following corollary.



(A) Elementary transformation on a surface



(B) Elementary transformation on the dual graph

FIGURE 2. Elementary transformations of trivalent graphs

Corollary 2.9. *Let γ be a trivalent graph, and c a coloring. Then the graph potential $\widetilde{W}_{\gamma,c}$ only depends on the homology class $[c] \in H_0(\gamma, \mathbb{F}_2)$, up to biregular automorphism of the torus.*

2.2. Elementary transformations. For a given surface of genus g there exist many (isotopy classes of) pair of pants decompositions. But they can be related via certain operations, which in [23, Appendix] are called (I), ..., (IV). It is remarked that (I) and (IV) in fact suffice to relate different decompositions for a surface, and that (IV) does not change the associated graph. Hence for our purposes we are only interested in the operation (I), which we will call an *elementary transformation*. Topologically this can be described as in Figure 2(a) on the surface and its dual graph in Figure 2(b).

For later reference we summarize the discussion from [23] as follows.

Proposition 2.10 (Hatcher–Thurston). *Elementary transformations act transitively on the set of colored trivalent graphs of genus g with n colored vertices, for $n = 0, \dots, 2g - 2$.*

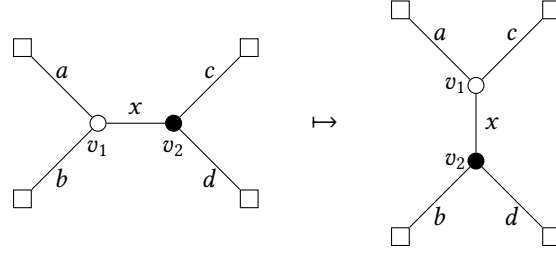
Elementary transformations will give us a family of mutations of Laurent polynomials, as discussed in [3]. We are mostly interested in the behavior of their periods under mutations induced by operations on the trivalent graph.

When considering the behavior of an elementary transformation of a trivalent graph on its associated graph potential, we can always split the graph potential as

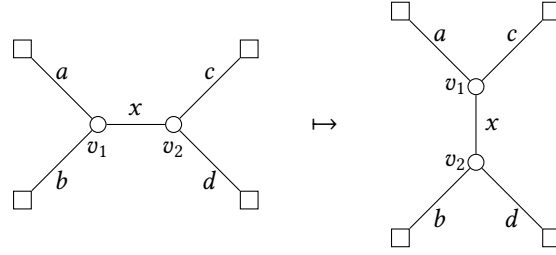
$$(37) \quad \widetilde{W}_{\gamma,c} = \widetilde{W}_{\gamma,c}^{\text{mut}} + \widetilde{W}_{\gamma,c}^{\text{frozen}}$$

where the mutated part involves the variables associated to the vertices v_1 and v_2 adjacent to the edge corresponding to the variable x . The frozen part of the graph potential is not changed, and can be ignored.

Elementary transformation with colors. Let us now describe how the graph potential changes when two edges attached to vertices of different colors come together, i.e. we consider Figure 3(a). We will denote by c the coloring of both γ and γ' , under the identification



(A) Elementary transformation with colors



(B) Elementary transformation without colors

FIGURE 3. Elementary transformations of trivalent graphs

of the vertices. Before the transformation we have

$$(38) \quad \begin{aligned} \widetilde{W}_{\gamma,c}^{\text{mut}} &= xcd + \frac{x}{cd} + \frac{d}{cx} + \frac{d}{cx} + \frac{1}{abx} + \frac{ab}{x} + \frac{ax}{b} + \frac{bx}{a} \\ &= \frac{1}{x} \left(ab + \frac{1}{ab} + \frac{c}{d} + \frac{d}{c} \right) + x \left(cd + \frac{1}{cd} + \frac{a}{b} + \frac{b}{a} \right). \end{aligned}$$

Denoting

$$(39) \quad \begin{aligned} \mu &:= \frac{1}{abcd} (c + abd)(d + abc) \\ \nu &:= \frac{1}{abcd} (a + bcd)(b + acd) \end{aligned}$$

we can write it as

$$(40) \quad \widetilde{W}_{\gamma,c}^{\text{mut}} = \frac{\mu}{x} + \nu x.$$

After the transformation we have

$$(41) \quad \begin{aligned} \widetilde{W}'_{\gamma,c}^{\text{mut}} &= x'bd + \frac{x'}{bd} + \frac{b}{dx'} + \frac{d}{bx'} + \frac{1}{acx'} + \frac{ac}{x'} + \frac{c}{ax'} + \frac{x'}{ac} \\ &= \frac{1}{x'} \left(ac + \frac{1}{ac} + \frac{b}{d} + \frac{d}{b} \right) + x' \left(bd + \frac{1}{bd} + \frac{a}{c} + \frac{c}{a} \right). \end{aligned}$$

Denoting

$$(42) \quad \begin{aligned} \mu' &:= \frac{1}{abcd} (b + acd)(d + acd) \\ \nu' &:= \frac{1}{abcd} (a + bcd)(c + abd) \end{aligned}$$

we can write it as

$$(43) \quad \widetilde{W}_{\gamma',c}^{\text{mut}} = \frac{\mu'}{x'} + v'x'.$$

Lemma 2.11. *Let μ, v, μ', v' be Laurent polynomials such that $\mu v = \mu' v'$. Then the Laurent polynomials $\frac{\mu}{x} + vx$ and $\frac{\mu'}{x'} + v'x'$ are identified after a rational change of coordinates.*

Proof. Setting $z = vx$ we have

$$(44) \quad \frac{\mu}{x} + vx = \frac{\mu v}{z} + z.$$

On the other hand we can do the rational change of coordinates $z = \frac{\mu'}{x'}$ to get

$$(45) \quad \frac{\mu}{x} + vx = \frac{\mu'}{x'} + \frac{\mu v x'}{\mu'}.$$

But by assumption we have $\frac{\mu v}{\mu'} = v'$, hence have identified $\frac{\mu}{x} + vx$ and $\frac{\mu'}{x'} + v'x'$. \square

Theorem 2.12. *Let γ and γ' be trivalent graphs related via an elementary transformation at an edge with different colors. Then*

- (1) *the graph potentials $\widetilde{W}_{\gamma,c}$ and $\widetilde{W}_{\gamma',c}$ are identified after a rational change of coordinates;*
- (2) *the rational transformation is invariant under the action of A_γ and $A_{\gamma'}$ and hence identifies $W_{\gamma,c}$ and $W_{\gamma',c}$.*

Proof. The first point follows from Lemma 2.11, as we have

$$(46) \quad \mu v = \mu' v' \frac{1}{(abcd)^2} (a + bcd)(b + acd)(c + abd)(d + abc).$$

Hence the rational transformation we are using is given by $x' = \frac{\mu'}{vx}$.

To prove the second point, observe that the group A_γ acts on the variables a, b, c, d, x via characters $\sigma_a, \sigma_b, \sigma_c, \sigma_d, \sigma_x$, satisfying the relations

$$(47) \quad \sigma_a \sigma_b = \sigma_x = \sigma_c \sigma_d.$$

Likewise $A_{\gamma'}$ acts on the variables a, b, c, d, x' via characters $\sigma'_a, \sigma'_b, \sigma'_c, \sigma'_d, \sigma'_{x'}$, satisfying the relations

$$(48) \quad \sigma'_a \sigma'_c = \sigma'_{x'} = \sigma'_b \sigma'_d.$$

To compute the action of A_γ and $A_{\gamma'}$ we write the rational change of coordinates more explicitly as

$$(49) \quad x' = \frac{(b + acd)(d + abc)}{x(a + bcd)(b + acd)}$$

where we have removed the factors $abcd$ (one coming from γ , the other from γ') as $\sigma_a \sigma_b \sigma_c \sigma_d$ and $\sigma'_a \sigma'_b \sigma'_c \sigma'_d$ are trivial so they do in fact cancel. The group $A_{\gamma'}$ acts on the numerator, the group A_γ on the denominator, and we need to check that for every $u \in A_\gamma \cong A_{\gamma'}$ the action on the left- and right-hand side agrees.

On the left-hand side we have that

$$(50) \quad u \cdot x' = \sigma'_{x'}(u)x'$$

whilst on the right-hand side we have that

$$(51) \quad u \cdot \frac{(b+acd)(d+abc)}{x(a+bcd)(b+acd)} = \frac{(\sigma'_b(u)b + \sigma'_a\sigma'_c\sigma'_d(u)acd) (\sigma'_d(u)d + \sigma'_a\sigma'_b\sigma'_c(u)abc)}{\sigma_x(u)x (\sigma_a(a) + \sigma_b\sigma_c\sigma_d(u)bcd) (\sigma_b(b) + \sigma_a\sigma_c\sigma_d(u)acd)}$$

$$= \frac{(\sigma'_b(u)b + \sigma'_b(u)acd) (\sigma'_d(u)d + \sigma'_d(u)abc)}{\sigma_x(u)x (\sigma_a(a) + \sigma_a(u)bcd) (\sigma_b(b) + \sigma_b(u)acd)}$$

$$= \frac{\sigma'_b\sigma'_d}{\sigma_x\sigma_a\sigma_b}(u) \frac{\mu'}{vx}.$$

But by the relations in (47) and (48) we have the necessary equality of characters. \square

Elementary transformations without colors. Let us now describe how the graph potential changes when two edges attached to vertices of the same colors (and hence it is enough to assume that they have no coloring) come together, i.e. we consider Figure 3(b). The proof is similar to the previous case, so not all details are given. Before the transformation we have

$$(52) \quad \widetilde{W}_Y^{\text{mut}} = xcd + \frac{x}{cd} + \frac{c}{dx} + \frac{d}{cx} + abx + \frac{a}{bx} + \frac{x}{ab} + \frac{b}{ax}$$

$$= \frac{1}{x} \left(\frac{a}{b} + \frac{b}{a} + \frac{c}{d} + \frac{d}{c} \right) + x \left(cd + \frac{1}{cd} + \frac{1}{ab} + ab \right).$$

Denoting

$$(53) \quad \mu := \frac{1}{abcd} (ad + bc)(ac + bd)$$

$$\nu := \frac{1}{abcd} (1 + abcd)(cd + ab)$$

we can write it as

$$(54) \quad \widetilde{W}_Y^{\text{mut}} = \frac{\mu}{x} + \nu x.$$

After the transformation we have

$$(55) \quad \widetilde{W}_Y^{\text{mut}} = x'bd + \frac{x'}{bd} + \frac{b}{dx'} + \frac{d}{bx'} + acx' + \frac{a}{cx'} + \frac{c}{ax'} + \frac{x'}{ac}$$

$$= \frac{1}{x'} \left(\frac{b}{d} + \frac{d}{b} + \frac{a}{c} + \frac{c}{a} \right) + x' \left(bd + \frac{1}{bd} + ac + \frac{1}{ac} \right).$$

Denoting

$$(56) \quad \mu' := \frac{1}{abcd} (ab + cd)(ad + bc)$$

$$\nu' := \frac{1}{abcd} (1 + abcd)(ac + bd)$$

we can write it as

$$(57) \quad \widetilde{W}_Y^{\text{mut}} = \frac{\mu'}{x'} + \nu' x'.$$

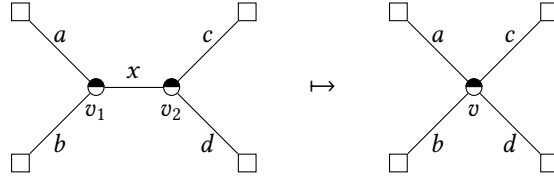


FIGURE 4. Edge contraction for an elementary transformation

We obtain the following analogue of Theorem 2.12, where we use that

$$(58) \quad \mu\nu = \mu'v' = \frac{1}{(abcd)^2} (1 + abcd)(ac + bd)(ab + cd)(ad + bc).$$

Theorem 2.13. *Let γ and γ' be trivalent graphs related via an elementary transformation at an edge with the same colors. Then*

- (1) *the graph potentials $\widetilde{W}_{\gamma,c}$ and $\widetilde{W}_{\gamma',c}$ are identified after a rational change of coordinates;*
- (2) *the rational transformation is invariant under the action of A_γ and $A_{\gamma'}$ and hence identifies $W_{\gamma,c}$ and $W_{\gamma',c}$.*

As a direct application of Theorem 2.12 and Theorem 2.13, we obtain the following corollary by tropicalizing the rational change of coordinates.

Corollary 2.14. *Let (γ, c) and (γ', c') be two trivalent colored graphs related by elementary transformations, then there are piecewise linear automorphisms $T_{\gamma,c}$ of \mathbb{R}^{3g-3} that maps*

$$(59) \quad T_{\gamma,c} : P_{\gamma,c} \rightarrow P_{\gamma',c'},$$

where $P_{\gamma,c}$ (resp. $P_{\gamma',c'}$) are the polar duals of the Newton polytope of $\widetilde{W}_{\gamma,c}$ (resp. $\widetilde{W}_{\gamma',c'}$).

Elementary transformations in terms of edge contractions. More conceptually we can describe these elementary transformations in terms of edge contractions and potentials for quadrivalent vertices.

We will consider Figure 3, and contract the edge x between the vertices v_1 and v_2 into a vertex v as in Figure 4. Associated to this vertex we add the variable z^\pm to the coordinate ring of the torus.

Let $v \in V$ be the quadrivalent vertex, and denote a, b, c, d the four edges incident to it. Then the *quadrivalent vertex potential* is the Laurent polynomial

$$(60) \quad \widetilde{W}_{v,c} := \begin{cases} \frac{(ab + cd)(ad + bc)(ac + bd)(1 + abcd)}{(abcd)^2} \frac{1}{z} + z & c(v) = 0 \\ \frac{(a + bcd)(b + acd)(c + abd)(d + abc)}{(abcd)^2} \frac{1}{z} + z & c(v) = 1. \end{cases}$$

Here the induced coloring $c(v)$ is defined as $c(v_1) + c(v_2)$.

Then the mutation of the graph potential can be described as the transformation

$$(61) \quad \widetilde{W}_{v_1,c} + \widetilde{W}_{v_2,c} \mapsto \frac{(ab + cd)(ad + bc)(ac + bd)(1 + abcd)}{(abcd)^2} \frac{1}{z} + z$$

if $c(v_1) + c(v_2) = c(v) = 0$, and

$$(62) \quad \widetilde{W}_{v_1, c} + \widetilde{W}_{v_2, c} \mapsto \frac{(a + bcd)(b + acd)(c + abd)(d + abc)}{(abcd)^2} \frac{1}{z} + z$$

if $c(v_1) + c(v_2) = c(v) = 1$.

2.3. Periods of Laurent polynomials. Consider an n -cycle $\{|x_1| = \dots = |x_n| = 1\}$ in the torus $(\mathbb{C}^\times)^n$, along with the normalized volume form $\left(\frac{1}{2\pi\sqrt{-1}}\right)^n \frac{dx_1}{x_1} \dots \frac{dx_n}{x_n}$.

Definition 2.15. Let $W \in \mathbb{C}[x_1^\pm, \dots, x_n^\pm]$ be a Laurent polynomial and denote by $[W]_0$ its constant term. The *period* $\pi_W(t)$ of W is defined as

$$(63) \quad \pi_W(t) := \left(\frac{1}{2\pi\sqrt{-1}}\right)^n \int \dots \int_{|x_1|=\dots=|x_n|=1} W \frac{dx_1}{x_1} \dots \frac{dx_n}{x_n},$$

which can be identified with

$$(64) \quad \pi_W(t) = \sum_{k \geq 0} [W^k]_0 t^k$$

for $t < 1/W(1)$.

We will often denote the constant term $[W^k]_0$ of the k th power of W as π_k . The inverse Laplace transform $\check{\pi}_W(t)$ of $\pi_W(t)$ is defined as

$$(65) \quad \check{\pi}_W(t) := \sum_{n \geq 0} \frac{[W^k]_0}{k!} t^k$$

The inverse Laplace transform $\check{\pi}_W(t)$ converges for all t and can also be written as

$$(66) \quad \check{\pi}_W(t) = \left(\frac{1}{2\pi\sqrt{-1}}\right)^n \int \dots \int_{|x_1|=\dots=|x_n|=1} \exp(tW) \frac{dx_1}{x_1} \dots \frac{dx_n}{x_n}.$$

Finally we remark that in Section 3, we will express $\pi_W(t)$ as the trace of a trace-class operator in the Hilbert space $\ell^2(\mathbb{Z})$.

In this way we have associated an integer sequence to a graph potential. Let us discuss the easiest example of this, where $g = 2$.

Example 2.16 (Genus two). The periods for the two colorings of the Theta graph as discussed in Example 2.6 are

$$(67) \quad \begin{aligned} \pi_{\widetilde{W}_{Y,0}}(t) &= 1 + 384t^4 + 645120t^8 + 1513881600t^{12} + \dots \\ \pi_{\widetilde{W}_{Y,c}}(t) &= 1 + 8t^2 + 216t^4 + 8000t^6 + 343000t^8 + 16003008t^{10} + 788889024t^{12} + \dots \end{aligned}$$

These are in fact the same as for the dumbbell graph, which will follow from Corollary 2.18.

The goal of this section is to prove that the periods of the graph potential only depend on the genus of the graph and the parity of the coloring. This will follow from the following lemma, which is a mild generalization of [3, Lemma 1], whose proof we include for completeness' sake.

Lemma 2.17. *Let φ be an automorphism of the field $\mathbb{C}(x_1, \dots, x_n)$ corresponding to a rational transformation of the torus $(\mathbb{C}^\times)^n = \text{Spec } \mathbb{C}[x_1^\pm, \dots, x_n^\pm]$, given by a collection of n rational functions $(p_1/q_1, \dots, p_n/q_n)$. Assume that for some $\alpha \in \mathbb{C}^\times$*

$$(68) \quad \varphi^* \omega = \alpha \omega,$$

where $\omega = d\log x_1 \wedge \dots \wedge d\log x_n$ is the volume form.

Let W, W' be Laurent polynomials in $\mathbb{C}[x_1^\pm, \dots, x_n^\pm]$. If $\varphi^*W = W'$, then $\pi_W(t) = \pi_{W'}(t)$.

Proof. Let Z_f be the vanishing locus of $f = \prod_{i=1}^n p_i q_i$. Consider the morphism

$$(69) \quad \text{Log}: (\mathbb{C}^\times)^n \rightarrow \mathbb{R}^n : (z_1, \dots, z_n) \mapsto (\log |z_1|, \dots, \log |z_n|).$$

By [21, Corollary 6.1.8] the image $A := \text{Log}(Z_f)$, called the *amoeba*, is a proper subset of \mathbb{R}^n , such that $\mathbb{R}^n \setminus A$ is a disjoint union of convex sets. There exists an element $r \in \mathbb{R}_{>0}^n$ such that φ is regular in all points of the torus

$$(70) \quad T_r := \{(z_1, \dots, z_n) \in (\mathbb{C}^\times)^n \mid \forall i = 1, \dots, n : |z_i| = r_i\} \subseteq U.$$

Here $U := (\mathbb{C}^\times)^n \setminus Z_f$. The cycles $T_r, T_{r'}$ are homologous in $(\mathbb{C}^\times)^n$ for any $r, r' \in \mathbb{R}_{>0}^n$, hence they define the same homology class in $H_n((\mathbb{C}^\times)^n, \mathbb{Z}) \cong \mathbb{Z}\gamma$, where $\gamma = [T_r]$.

This implies that $[\varphi(T_r)] = k\gamma \in H_n(T, \mathbb{Z})$ for some $k \in \mathbb{Z}$. But we also see that

$$(71) \quad \alpha = \alpha \int_{T_r} \omega = \alpha \int_{T_r} i_U^*(\omega_U) = \int_{T_r} \varphi_U^*(\omega_U) = \int_{\varphi(T_r)} \omega = \int_{kT_{r'}} \omega = k$$

where $i_U: U \rightarrow (\mathbb{C}^\times)^n$ and φ_U is the composition of the rational map φ with i_U , which is everywhere defined. Hence $\alpha = k$ is a non-zero integer.

Now for any $r \in \mathbb{R}_{>0}^n$ such that $T_r \subseteq U$ the equality

$$(72) \quad \alpha \int_{T_r} \frac{\omega}{1-tW'} = \int_{T_r} \varphi^* \left(\frac{\omega}{1-tW} \right) = \int_{\varphi(T_r)} \frac{\omega}{1-tW} = k \int_{T_r} \frac{\omega}{1-tW}$$

and non-vanishing of $\alpha = k$ implies the equality of periods. \square

Hence we obtain the following corollary.

Corollary 2.18. *Let (γ, c) and (γ', c') be related via elementary transformations or change of colors by the boundary of a 1-chain $C_1(\gamma, \mathbb{F}_2)$. Then their periods agree, i.e.*

$$(73) \quad \pi_{\overline{W}_{\gamma, c}}(t) = \pi_{\overline{W}_{\gamma', c'}}(t).$$

and moreover are independent of the choice of ambient lattice, i.e.

$$(74) \quad \pi_{\overline{W}_{\gamma, c}}(t) = \pi_{W_{\gamma, c}}(t),$$

This explains why in Example 2.16 we could claim that the periods for the two distinct genus two graphs agree. And combining the corollary with Proposition 2.10 we have that the periods only depend on the genus and the parity of the coloring.

3. TOPOLOGICAL QUANTUM FIELD THEORIES FROM GRAPH POTENTIALS

The invariance under elementary transformations from Section 2.2 can be used to define a two-dimensional topological quantum field theory (or 2d TQFT for short), which will give an efficient computational tool to compute period sequences. Let us quickly recall what 2d TQFTs are, using the functorial description from Atiyah [5].

A *two-dimensional topological quantum field theory* is a symmetric monoidal functor

$$(75) \quad Z: (\text{Bord}_2, \sqcup) \rightarrow (\mathcal{C}, \otimes)$$

from the symmetric monoidal category Bord_2 of 2-bordisms to a symmetric monoidal category (\mathcal{C}, \otimes) . An object in Bord_2 is an oriented closed curve (a closed topological

manifold of real dimension one), i.e. a (possibly empty) disjoint union of copies of S^1 , and a morphism (or bordism) from E to F is an equivalence class of oriented compact surfaces M together with identifications of the boundary ∂M to E and F . The equivalence relation identifies bordisms via orientation-preserving diffeomorphisms, keeping only the topological information. We will write S_0^1 (respectively S_1^1) for the circle with anticlockwise (respectively clockwise) orientation.

3.1. Restricted TQFT. For our purposes, we will take as our target category the category of real Hilbert spaces (not necessarily finite-dimensional), with the space of bounded operators between Hilbert spaces as morphisms. This category is a monoidal category under the *Hilbertian tensor product* but it is not rigid. As rigidity implies the existence of the trace function for all endomorphisms which forces the Hilbert spaces to be finite-dimensional. This also means that we cannot consider the traces of the identity operator as in [5, page 180], and hence we must not consider cups and caps.

However to every Hilbert space \mathcal{H} , we can consider its continuous dual \mathcal{H}^* which is linearly isomorphic to \mathcal{H} . Moreover, this gives a natural linear isomorphism between the Hilbertian tensor product $\mathcal{H}_1 \otimes \mathcal{H}_2$ and the space of Hilbert–Schmidt operators $\text{HS}(\mathcal{H}_1^*, \mathcal{H}_2)$.

The category of Hilbert spaces has additional structure, by the Riesz representation theorem. Namely, to every bounded operator $f : \mathcal{H}_1 \rightarrow \mathcal{H}_2$ we can assign the adjoint operator $f^* : \mathcal{H}_2 \rightarrow \mathcal{H}_1$ of a morphism, which satisfies the following properties:

- (1) $\text{Id}^* = \text{Id}$;
- (2) $(f \circ g)^* = g^* \circ f^*$;
- (3) $f^{**} = f$.

Categories with morphisms satisfying the above conditions are known as **-categories*. The category Bord_2 is naturally a **-category* as to every bordism we can assign the opposite bordism.

If M is an object in Bord_2 and \overline{M} is the surface M with opposite orientation, and we take our target category as the category of Hilbert spaces as above, then $Z(M)$ is finite-dimensional. This follows from the existence of both the evaluation map $\text{Hom}_{\text{Bord}_2}(\overline{M} \sqcup M, \emptyset)$ and the coevaluation map, which implies that the vector space $Z(M)$ has a rigid dual, see for example [29, Proposition 1.1.8].

Hence to allow infinite-dimensional spaces we also need to slightly modify our source category, by *discarding* some bordisms in Bord_2 while the objects remain the same. The new category will be denoted by RBord_2 . Namely we will only consider bordisms given by surfaces $\Sigma_{g,n}$ (where g is the genus and n the number of boundary components) for which the Euler characteristic $2 - 2g - n$ is strictly negative, together with cylinders (to ensure we have identity morphisms), braidings and handles considered as elements of $\text{Hom}_{\text{RBord}_2}(S^1 \sqcup S^1, \emptyset)$. This will then suffice to define invariants of closed surfaces of genus $g \geq 2$.

We have thus defined RBord_2 as a non-full subcategory of Bord_2 . Observe that by the symmetries inherent in the definition of these TQFT's (see Lemmas 3.6 and 3.8), the pair of pants $\Sigma_{0,3}$ appears as a morphism $S^1 \sqcup S^1 \rightarrow S^1$ and $S^1 \rightarrow S^1 \sqcup S^1$ with the appropriate orientations, but also as a morphism $S^1 \sqcup S^1 \sqcup S^1 \rightarrow \emptyset$ and $\emptyset \rightarrow S^1 \sqcup S^1 \sqcup S^1$.

Remark 3.1. The category RBord_2 is not a $*$ -category. Observe that we are not allowing opposite handles (nor cups or caps) in the morphisms $\text{Hom}_{\text{RBord}_2}(\emptyset, S^1 \sqcup S^1)$ in the restricted bordisms category RBord_2 . A handle combined with an opposite handle gives a torus whose corresponding assignment is the trace of the identity operator. Since our target category is the category of Hilbert spaces, the trace of identity may not be defined. This is one of the main reasons for considering the restricted bordism category RBord_2 .

In fact, we will describe a *family* of 2d TQFT's, parametrized by $t \in \mathbb{R}$. It is only by considering the entire family of TQFT's that we can efficiently compute period sequences.

Remark 3.2. Two-dimensional TQFT's (with values in finite-dimensional vector spaces) can equivalently be described using Frobenius algebras [16, 2]. Because we consider a more general target category, and restricted the possible bordisms, we do not get the usual notion of a unital Frobenius algebra, but rather we get a Hilbertian algebra. The algebra structure on $\ell^2(\mathbb{Z})$ with an associated Spin-structure, in the sense of [40] should be analyzed. We leave this for future work.

3.2. The graph potential TQFT. We fix $t \in \mathbb{R}$. Using graph potentials we will construct a TQFT with values in Hilbert spaces for every value of t .

Later we will allow t to vary, *after* we have made the identification ensuring that at least the partition function for surfaces without punctures is related to the period of a graph potential, and therefore is well-behaved when we let t vary. This suffices for our purposes.

Witten–Dijkgraaf–Verlinde–Verlinde (WDVV) equations. We can describe a 2d TQFT in terms of the WDVV equations. For this, let $(\mathcal{H}, \langle -, - \rangle)$ be a Hilbert space. This will be the value of our 2d TQFT for S_e^1 , and later on we will take it to be $\ell^2(\mathbb{Z})$.

We have a multilinear form $\langle -, - \rangle^{\otimes n} : \mathcal{H}^{\otimes n} \rightarrow \mathbb{R}$ for all $n \geq 1$, and a natural pairing $\langle -, - \rangle_{i,j} : \mathcal{H}^{\otimes n} \rightarrow \mathcal{H}^{\otimes n-2}$ for all $i < j$ by pairing the i th and j th factor.

Consider an assignment $\mathcal{M}_3(t) = \mathcal{M}_3(t; i, j, k) \in \mathcal{H}^{\otimes 3}$, where we will use i, j, k to refer to the three tensor factors. This labeling allows us to refer to specific factors in repeated tensor products of the element $\mathcal{M}_3(t)$.

Assume that $\mathcal{M}_3(t)$ is symmetric in its factors. Then we can define the assignment

$$(76) \quad \mathcal{M}_4(t) = \mathcal{M}_4(t; i, j, k, l) := \langle -, - \rangle_{m,n} (\mathcal{M}_3(t; i, j, m) \otimes \mathcal{M}_3(t; k, l, n)) \in \mathcal{H}^{\otimes 4}.$$

Here $\langle -, - \rangle_{m,n}$ refers to the natural pairing of the third and sixth factor.

Definition 3.3. We say that $\mathcal{M}_3(t) \in \mathcal{H}^{\otimes 3}$ is a *solution to the WDVV equation* if the tensor $\mathcal{M}_4(t) \in \mathcal{H}^{\otimes 4}$ is symmetric in i, j, k, l .

Let $\mathcal{M}_3(t)$ be such an assignment which satisfies the WDVV equation. Then we can construct a 2d TQFT as follows.

Construction 3.4. Let $\Sigma_{g,n}$ be an oriented surface of genus g with n punctures, such that $2 - 2g - n < 0$. For every pair of pants, we will consider its dual graph. This is an oriented trivalent graph with one vertex and three half-edges. If the boundary circle is oriented anticlockwise i.e. S_0^1 , then the half-edge is oriented outwards and vice versa as shown in Figure 5.

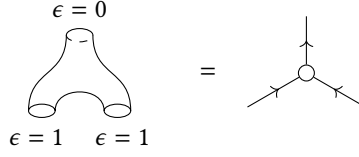


FIGURE 5. Dual graph to oriented pair of pants



FIGURE 6. Labeling for internal edges and trivalent vertices

By choosing a pair of pants decomposition of $\Sigma_{g,n}$ we assign the dual graph γ . Observe that γ has oriented half-edges and internal edges are unoriented. We can assign

$$(77) \quad \mathcal{M}_{\Sigma_{g,n}}(t) := \bigotimes_{e \in E_{\text{int}}} \langle -, - \rangle_{a,b} \left(\bigotimes_{v \in V} \mathcal{M}_3(t; i, j, k) \right) \in \mathcal{H}^{\otimes n}$$

where we use the labeling for internal edges and trivalent vertices as in Figure 6, and the tensor product over the internal edges means we apply all possible pairings $\langle -, - \rangle_{a,b}$ where the vertices a and b refer to specific factors in the tensor product $\bigotimes_{v \in V} \mathcal{M}_3(t; i, j, k)$.

Using the relationship between 2d TQFT's and solutions to the WDVV equation (see e.g. [20, §9], where the WDVV equation is referred to as the associativity equation) we obtain the following result.

Proposition 3.5. *Let $\mathcal{M}_3(t) \in \mathcal{H}^{\otimes 3}$ be a solution to the WDVV equations. Then Construction 3.4 is independent of the choice of the pair of pants decomposition.*

Graph potentials as solutions to the WDVV equations. Now we will revisit the setting introduced in the introduction, in particular the functional equation in (1) and the ensuing discussion. We set \mathcal{H} to be $\ell^2(\mathbb{Z})$. By Fourier expansion, any $f \in \ell^2(\mathbb{Z})$ can be written as

$$(78) \quad \sum_{i \in \mathbb{Z}} a_i z^i,$$

where the collection $\{z^i\}_{i \in \mathbb{Z}}$ is a complete orthonormal basis of $\ell^2(\mathbb{Z})$ with respect to the standard pairing on $\ell^2(\mathbb{Z})$ given by

$$(79) \quad \begin{aligned} \langle f(z), g(z) \rangle_z &= \left\langle \sum_{i \in \mathbb{Z}} a_i z^i, \sum_j b_j z^j \right\rangle_z \\ &= \sum_{i \in \mathbb{Z}} a_i b_i \\ &= \frac{1}{2\pi\sqrt{-1}} \int_{S^1} f(z) g(z^{-1}) \frac{dz}{z}. \end{aligned}$$

The WDVV equation can be rephrased as follows in this particular setting. Consider a $f(x_1, x_2, x_3) \in \ell^2(\mathbb{Z})^{\otimes 3}$. Assume now that there exists a function φ such that

$$(80) \quad f(x_1, x_2, y)f(x_3, x_4, y) = f(x_1, x_3, z)f(x_2, x_4, z)$$

in $\ell^2(\mathbb{Z})^{\otimes 6}$, where $y = \varphi(z, x_1, x_2, x_3, x_4)$ is a function such that the Jacobian of φ is the identity. In that case we get that $\varphi_* \frac{dz}{z} = \frac{dy}{y}$, and hence

$$(81) \quad \begin{aligned} \langle f(x_1, x_2, y) \otimes f(x_3, x_4, y^{-1}) \rangle_y &= \int_{S^1} f(x_1, x_2, y)f(x_3, x_4, y) \frac{dy}{y} \\ &= \int_{S^1} f(x_1, x_3, z)f(x_2, x_4, z) \frac{dz}{z} \\ &= \langle f(x_1, x_3, z) \otimes f(x_2, x_4, z^{-1}) \rangle_z \end{aligned}$$

in $\ell^2(\mathbb{Z})^{\otimes 4}$ giving a solution to the WDVV equation. Taking the logarithm of the function f we can interpret the multiplicative condition as an *additive* condition, and this brings us in the setting of Section 2.

In (26) we have defined the vertex potential at a vertex $v \in V$ of a colored graph (γ, c) . Using the variables x, y, z , and writing $\epsilon = c(v)$ we have that

$$(82) \quad \widetilde{W}_{v,\epsilon} = (xyz)^{(-1)^\epsilon} + (xy^{-1}z^{-1})^{(-1)^\epsilon} + (x^{-1}yz^{-1})^{(-1)^\epsilon} + (x^{-1}y^{-1}z)^{(-1)^\epsilon}.$$

We observe that $\widetilde{W}_{v,\epsilon}$ is symmetric in the variables x, y, z . We also have the following symmetries, aside from the symmetry in the variables.

Lemma 3.6. *The vertex potential satisfies*

$$(83) \quad \begin{aligned} \widetilde{W}_{v,0}(x, y, z) &= \widetilde{W}_{v,0}(x^{-1}, y^{-1}, z) \\ &= \widetilde{W}_{v,1}(x^{-1}, y, z) \\ \widetilde{W}_{v,1}(x, y, z) &= \widetilde{W}_{v,0}(x^{-1}, y, z) \\ &= \widetilde{W}_{v,0}(x^{-1}, y^{-1}, z^{-1}). \end{aligned}$$

Definition 3.7. Let ϵ be 0 or 1, and $t \in \mathbb{R}$. We define

$$(84) \quad \begin{aligned} f_\epsilon(x, y, z; t) &:= \exp\left(t \widetilde{W}_{v,\epsilon}(x, y, z)\right) \\ &= \sum_{a,b,c,d \geq 0} \frac{t^{a+b+c+d}}{a!b!c!d!} x^{(-1)^\epsilon((a+b)-(c+d))} y^{(-1)^\epsilon((a+c)-(b+d))} z^{(-1)^\epsilon((a+d)-(b+c))}. \end{aligned}$$

The following lemma follows directly.

Lemma 3.8. *For all $t \in \mathbb{R}$ we have that $f_\epsilon(x, y, z; t) \in \ell^2(\mathbb{Z})^{\otimes 3}$. It is moreover symmetric in x, y, z .*

Finally, as observed above, we have translated between an additive and a multiplicative form of the WDVV equation, and hence by Section 2.2 we obtain the following

Proposition 3.9. *For all $t \in \mathbb{R}$ we have that $f_\epsilon(x, y, z; t)$ satisfies the WDVV equation.*

We now come to the essential construction.

Construction 3.10. Let $t \in \mathbb{R}$. The *graph potential field theory* $Z^{\text{gp}}(t)$ for t is defined as follows.

Let $\Sigma_{0,3;\epsilon_1,\epsilon_2,\epsilon_3}$ be a pair of pants, and $\epsilon_1, \epsilon_2, \epsilon_3$ denote the orientation of the three boundary circles. Let γ be the trivalent graph on one vertex and three oriented half-edges which is dual to the pair of pants. Then we define the partition function as

$$(85) \quad Z^{\text{gp}}(t)(\Sigma_{0,3;\epsilon_1,\epsilon_2,\epsilon_3}) := \exp\left(t\tilde{W}_{v,0}(x^{(-1)\epsilon_1}, y^{(-1)\epsilon_2}, z^{(-1)\epsilon_3})\right)$$

in $\ell^2(\mathbb{Z})^{\otimes 3}$. Here v is the unique vertex of the dual graph γ of $\Sigma_{0,3;\epsilon_1,\epsilon_2,\epsilon_3}$. We assign x, y, z (resp. x^{-1}, y^{-1}, z^{-1}) as coordinate variables corresponding to the half-edges that are oriented outwards (resp. inwards) as shown in Figure 7.

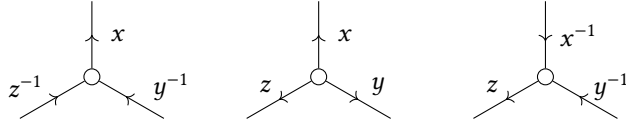


FIGURE 7. Variable attachment to oriented graphs

The assignment to the oriented pair of pants is well-defined by virtue of Lemma 3.6. Moreover Lemma 3.6 also implies that

$$(86) \quad Z^{\text{gp}}(t)(\Sigma_{0,3;\epsilon_1,\epsilon_2,\epsilon_3}) = \exp\left(t\tilde{W}_{v,\epsilon}(x, y, z)\right),$$

where $\epsilon = \epsilon_1 + \epsilon_2 + \epsilon_3$.

Hence all the graphs shown in Figure 7 have the same partition function $\exp\left(t\tilde{W}_{v,0}(x, y, z)\right)$. Similarly all the graphs in Figure 8 have the same partition function $\exp\left(t\tilde{W}_{v,1}(x, y, z)\right)$.

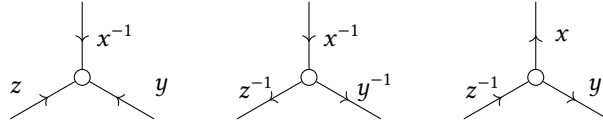


FIGURE 8. Variable attachment to oppositely oriented graphs

This is an additional feature of our partition function and we color the vertex of γ with color $\epsilon = \epsilon_1 + \epsilon_2 + \epsilon_3$ to mark this feature.

To the cylinder in $\text{Hom}_{\text{RBord}_2}(S_\epsilon^1, S_{\epsilon+1}^1)$ we assign the identity morphism in $\text{End}(\ell^2(\mathbb{Z}))$, and similarly for any braiding we just assign the identity morphism on all the factors. The handle in $\text{Hom}_{\text{RBord}_2}(S_\epsilon^1 \sqcup S_{\epsilon+1}^1, \emptyset)$ is assigned the evaluation map which is also natural pairing on the Hilbert space $\ell^2(\mathbb{Z})$.

Let $\Sigma_{g,n}$ be a connected oriented surface of genus g with n boundary components satisfying $2 - 2g - n < 0$. Consider a pair of pants decomposition for $\Sigma_{g,n}$, and let γ be the trivalent dual graph with n half-edges determined by the pair of pants decomposition. We incorporate the orientation of $\Sigma_{g,n}$ as follows. Cut γ along the internal edges E_{int} to form a forest consisting of $2g - 2$ trivalent graphs with one vertex and three half-edges with

appropriate orientations. The coloring of the vertices is determined by the parity of the orientations of the number of clockwise circles of each pair of pants. We set

$$(87) \quad Z^{\text{sp}}(t)(\Sigma_{g,n}) := \bigotimes_{e \in E_{\text{int}}} \langle -, - \rangle_{a,b} \left(\bigotimes_{v \in V} \exp \left(t \tilde{W}_{v,\epsilon}(x, y, z) \right) \right)$$

in $\ell^2(\mathbb{Z})^{\otimes n}$. As in (77), we use the labeling for internal edges and trivalent vertices as in Figure 6, and the tensor product over the internal edges means we apply all possible pairings $\langle -, - \rangle_{a,b}$ where the vertices a and b refer to specific factors in the tensor product indexed by the set of vertices of V .

By (85), (86) and Lemma 3.6, we get

$$(88) \quad W_{v,0}(x^{(-1)\epsilon_1}, y^{(-1)\epsilon_2}, z^{(-1)\epsilon_3}) = W_{v,0}(x^{(-1)\epsilon_1}, y^{(-1)\epsilon_2+1}, z^{(-1)\epsilon_3+1}).$$

Equating the variables y and z and taking inner product in the variable y , we get

$$(89) \quad \langle W_{v,0}(x^{(-1)\epsilon_1}, y^{(-1)\epsilon}, y^{(-1)\epsilon+1}) \rangle_y = \langle W_{v,0}(x^{(-1)\epsilon_1}, y^{(-1)\epsilon+1}, y^{(-1)\epsilon}) \rangle_y$$

This equality encodes that we obtain the same partition function for one-holed torus with decompositions obtained from cutting and gluing with two different circles as shown in Figure 9. Thus the partition function $Z^{\text{sp}}(t)(\Sigma_{1,1})$ for a one-holed torus is well-defined.

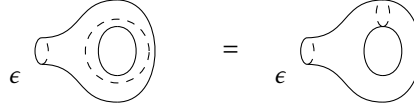


FIGURE 9. Fundamental relation for one-holed torus

Hence by Proposition 3.5, the fact that cylinders and braidings are the identity, and that the handle is assigned the natural pairing, we obtain the following

Corollary 3.11. *For all $t \in \mathbb{R}$, the assignment $Z^{\text{sp}}(t)$ defines a two-dimensional TQFT on the restricted bordism category RBord_2 .*

This proves Theorem B.

It would be interesting to formalize this notion of a family of infinite-dimensional TQFT's, so that one can consider all of them together. We will not develop such a formalism. Rather we will only consider the family of partition functions for closed surfaces, defined by this TQFT. This will allow us in Section 4 to obtain an efficient method to compute periods of graph potentials.

4. COMPUTING PERIODS VIA THE GRAPH POTENTIAL TQFT

We can now turn our discussion to a practical method to compute the periods of graph potentials using topological quantum field theories. We also refer to [14, 15] for various interesting interpretations of periods, and the use of infinite-dimensional Hilbert spaces (albeit using different methods) to compute them.

The following definition extends Definition 2.3, where we now allow leaves (or half-edges) to be present in the graph, as the definition of the vertex potentials does not depend on whether we have half-edges or not.



FIGURE 10. Cutting an internal edge

Definition 4.1. Let (γ, c) be a colored trivalent graph of genus g with n leaves. We define the *graph potential* $\widetilde{W}_{\gamma, c}$ as the sum of vertex potentials.

For a graph with half-edges we let E_{int} denote the set of internal edges, i.e. we remove any half-edges from E . Let us enumerate the variables associated to internal edges E_{int} as x_1, \dots, x_{3g-3+n} . We introduce the following notation.

Notation 4.2. Let (γ, c) be a colored trivalent graph of genus g with n leaves such that $2 - 2g - n < 0$. Orient the half-edges of γ such that half-edges attached to vertices v of color $c(v) = 0$ are pointing outwards while those attached to vertices of $c(v) = 1$ are pointing inwards. This orientation is consistent with the orientation coming from pair of pants decomposition.

Denote by

$$(90) \quad \mathcal{K}_{\gamma, c}(t) := \left(\frac{1}{2\pi\sqrt{-1}} \right)^{\#E_{\text{int}}} \int \cdots \int_{(S^1)^{E_{\text{int}}}} \exp\left(t \widetilde{W}_{\gamma, c}(x_1, \dots, x_{3g-3+n})\right) \frac{dx_1}{x_1} \cdots \frac{dx_{3g-3+n}}{x_{3g-3+n}}$$

the corresponding element of $\ell^2(\mathbb{Z})^{\otimes n}$.

We record the following important observation as a lemma.

Lemma 4.3. *If $n = 0$, then (90) reduces to*

$$(91) \quad \mathcal{K}_{\gamma, c}(t) = \widetilde{\pi}_{\widetilde{W}_{\gamma, c}}(t)$$

where $\widetilde{\pi}_{\widetilde{W}_{\gamma, c}}(t)$ is the inverse Fourier–Laplace transform of the period $\pi_{\widetilde{W}_{\gamma, c}}(t)$ of the graph potential.

In other words, if $\pi_{\widetilde{W}_{\gamma, c}}(t) = \sum_{n \geq 0} \pi_n t^n$, then $\mathcal{K}_{\gamma, c}(t) = \sum_{n \geq 0} p_n t^n$, where $p_n = \pi_n/n!$.

We have the following proposition, which follows from the change of variables formula for integrals. It is an important computational tool in what follows.

Proposition 4.4. *Let γ' be a trivalent graph with $n + 2$ leaves. Let c be a coloring. Consider half-edges e' and e'' adjacent to vertices a and b . We define a new colored trivalent graph γ (with n leaves) by replacing two leaves at the vertices a and b by the internal edge e connecting a and b , as in Figure 10. Then*

$$(92) \quad \mathcal{K}_{\gamma, c}(t) = \frac{1}{2\pi\sqrt{-1}} \int_{S^1} \mathcal{K}_{\gamma', c}(t)|_{x_{e'}=x_{e''}=z} \frac{dz}{z}.$$

where $x_{e'}$ and $x_{e''}$ are variables associated to the leaves e' and e'' attached to the vertices a and b .

Observe that not all trivalent colored graphs that we considered in Section 2 arise as the dual graph of a pair of pants decomposition of an orientable surface whose boundary has induced orientations. Since the category RBord_2 only consists of objects of this form, we

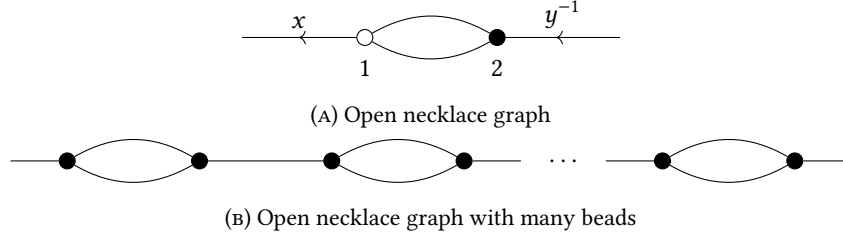


FIGURE 11. Necklace graphs

need the following results to use the TQFT partition function $Z^{\text{sp}}(t)$ effectively to compute periods of arbitrary (γ, c) .

The following proposition relates $\mathcal{K}_{\gamma,c}(t)$ to the partition function of the $\ell^2(\mathbb{Z})$ -valued TQFT that we constructed.

Proposition 4.5. *Let $\Sigma_{g,n}$ be a oriented surface of genus g with n boundary components and let (γ, c) be the dual graph obtained from a pair of pants decomposition of $\Sigma_{g,n}$. If $3g - 3 + n$ is even, then*

$$(93) \quad \mathcal{K}_{\gamma,c}(t) = Z^{\text{sp}}(t)(\Sigma_{g,n}).$$

Proof. Proposition 4.4 allows us to write $\mathcal{K}_{\gamma,c}(t)$ as the iterated integral over the pair of pants decomposition. Since we need $3g - 3 + n$ cuts to get to the pair of pants, the parity being even guarantees that we can use Lemma 3.6 to match up the integral with the norms in $\ell^2(\mathbb{Z})$ that appears in the definition of $Z^{\text{sp}}(t)(\Sigma_{g,n})$. \square

Remark 4.6. If $3g - 3 + n$ is odd, then we can compute $\mathcal{K}_{\gamma,c}(t)$ by first cutting (γ, c) along one edge to produce a new graph (γ', c') , and then use Proposition 4.5 for (γ', c') and apply Proposition 4.4.

Bessel functions. To adequately work with the partition functions of this topological quantum field theory we recall that the modified Bessel function of the second kind is defined as

$$(94) \quad I_\alpha(z) := \sum_{m \geq 0} \frac{1}{m! \Gamma(m + \alpha + 1)} \left(\frac{z}{2}\right)^{2m + \alpha}.$$

For our purposes we are only interested in the case $\alpha = 0$, with a rescaling of the argument. We will use the following notation.

Notation 4.7. We denote

$$(95) \quad B(z) := I_{\alpha=0}(2z) = \sum_{m \geq 0} \frac{1}{(m!)^2} z^{2m}.$$

The following lemma explains why this function is relevant to us. It allows us to give an explicit expression for the partition function for the open necklace graph $\gamma_{1,2}$ from Figure 11(a). The necklace graph is the dual graph of the two-holed torus as shown in Figure 12

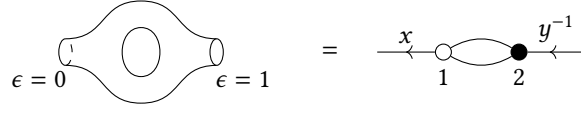


FIGURE 12. Dual graph of the two-holed torus

Lemma 4.8. *Let $\gamma = \gamma_{1,2}$ be the open necklace graph as in Figure 11(a), with one half-edge oriented outwards and the other one oriented inwards. Then*

$$(96) \quad \mathcal{K}_{\gamma,1}(t) = B(t(x + y^{-1})) B(t(x^{-1} + y)).$$

Proof. The colored graph $(\gamma, 1)$ in the statement of the lemma is the dual graph obtained from a pair of pants decomposition of a two-holed torus with one hole oriented anticlockwise and the other one oriented clockwise. This is obtained by gluing two pairs of pants as shown in Figure 13.

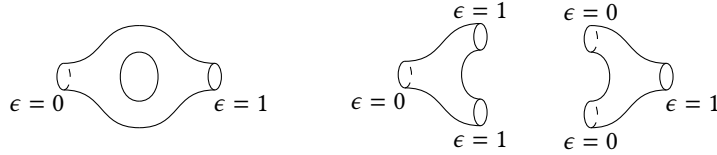


FIGURE 13. Pants decomposition for the two-holed torus

Now the graph $\gamma_{1,2}$ is obtained two half-edges of a trivalent graph with one vertex as shown in Figure 14

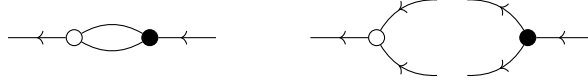


FIGURE 14. Genus one graph from gluing

By definition, Proposition 4.5, and (77), we have

(97)

$$(98) \quad \mathcal{K}_{\gamma,1}(t) = \left\langle \exp(t(\tilde{W}_{v,0}(x, u^{-1}, v^{-1}) + \tilde{W}_{v,0}(y^{-1}, u, v))) \right\rangle_{u,v}$$

$$= \frac{1}{(2\pi\sqrt{-1})^2} \iint_{S^1 \times S^1} \exp(t(\tilde{W}_{v,0}(x, u^{-1}, v^{-1}) + \tilde{W}_{v,0}(y^{-1}, u^{-1}, v^{-1}))) \frac{du}{u} \frac{dv}{v}$$

$$(99) \quad = \frac{1}{(2\pi\sqrt{-1})^2} \iint_{S^1 \times S^1} \exp(t(\tilde{W}_{v,0}(x, u, v) + \tilde{W}_{v,0}(y^{-1}, u, v))) \frac{du}{u} \frac{dv}{v}$$

which we can interpret as

$$(100) \quad = [\exp(t(\tilde{W}_{v,0}(x, u, v) + \tilde{W}_{v,0}(y^{-1}, u, v)))]_{u^0 v^0}.$$

Via the following sequence of rewrites

$$(101) = \sum_{\substack{a,b,c,d,a',b',c',d' \\ b+d+b'+d'=a'+c'+a+c \\ a'+d'+a+d=b+c+b'+c'}} \frac{t^{(a+b+c+d)+(a'+b'+c'+d')}}{a!a'!b!b'!c!c'!d!d'!} x^{(a+b)-(c+d)} y^{-(a'+b')+(c'+d')}$$

$$(102) = \sum_{\substack{a,b,c,d,a',b',c',d' \\ c+c'=d+d' \\ a+a'=b+b'}} \frac{t^{(a+b+c+d)+(a'+b'+c'+d')}}{a!a'!b!b'!c!c'!d!d'!} x^{(a+b)-(c+d)} y^{-(a'+b')+(c'+d')}$$

$$(103) = \sum_{\substack{a_1,b_1,c_1,d_1,a,a',c,c' \\ c_1+d_1=2(c+c') \\ a_1+b_1=2(a+a')}} \frac{t^{a_1+b_1+c_1+d_1}}{a!(a_1-a)!a'!(b_1-a')!c!(c_1-c)!c'!(d_1-c)!} x^{a_1-c_1} y^{-b_1+d_1}$$

$$(104) = \sum_{m,n} \sum_{\substack{a_1,b_1,c_1,d_1,a,c \\ a \leq m, c \leq n \\ c_1+d_1=2n; a_1+b_1=2m}} \frac{t^{2(m+n)}}{a!(a_1-a)!a'!(b_1-a')!c!(c_1-c)!c'!(d_1-c)!} x^{a_1-c_1} y^{-b_1+d_1}$$

$$(105) = \sum_{m \geq 0, n \geq 0} \sum_{\substack{a_1,b_1,c_1,d_1,a,c \\ a \leq m, c \leq n \\ c_1+d_1=2n; a_1+b_1=2m}} \frac{t^{2(m+n)}}{a_1!b_1!c_1!d_1!} x^{a_1-c_1} y^{-b_1+d_1} \binom{a_1}{a} \binom{b_1}{m-a} \binom{c_1}{c} \binom{d_1}{n-c}$$

$$(106) = \sum_{m \geq 0, n \geq 0} \sum_{\substack{a_1,b_1,c_1,d_1 \\ a_1+b_1=2m; c_1+d_1=2n}} t^{2(m+n)} \binom{2m}{m} \binom{2n}{n} \frac{x^{a_1-c_1} (y^{-1})^{b_1-d_1}}{a_1!b_1!c_1!d_1!}$$

we finally obtain

$$(107) = B(t(x+y^{-1})) B(t(x^{-1}+y))$$

as desired. \square

As a direct corollary of Lemma 4.3 and Remark 4.6 we obtain

Corollary 4.9. *Let $\gamma = \gamma_{1,2}$ be the graph $\gamma_{1,2}$ with no colored vertices, then*

$$(108) \quad \mathcal{K}_{\gamma,0}(t) = B(t(x+y)) B(t(x^{-1}+y^{-1})).$$

Before we discuss the general case, we will give a formula in the genus two case. This formula will be revisited in [10, Appendix B]

Corollary 4.10. *Let γ be a genus two graph, without half-edges. We consider the case $\epsilon = 1$. Then the inverse Fourier–Laplace transform of the period $\pi_{\overline{W}_{\gamma,\epsilon}}(t)$ is given by*

$$(109) \quad \sum_{n \geq 0} \frac{(2n!)^2}{n!^6} t^{2n}.$$

Proof. If we cut the colored graph $(\gamma, 1)$ along any edge then we get back the graph considered in Lemma 4.3. Hence, by Lemma 4.3, (77), and Lemma 4.8, we have putting

after $x = y$

$$\begin{aligned}
(110) \quad & \widetilde{\pi}_{\widetilde{W}_{y,1}}(t) \\
&= \sum_{m \geq 0, n \geq 0} \sum_{\substack{a_1, b_1, c_1, d_1 \\ a_1 + b_1 = 2m; c_1 + d_1 = 2n}} t^{2(m+n)} \binom{2m}{m} \binom{2n}{n} \frac{1}{a_1! b_1! c_1! d_1!} \left(\frac{1}{2\pi\sqrt{-1}} \int_{S^1} x^{a_1 - c_1} \cdot (x^{-1})^{b_1 - d_1} \frac{dx}{x} \right) \\
&= \sum_{m \geq 0, n \geq 0} \sum_{\substack{a_1, b_1, c_1, d_1 \\ a_1 + b_1 = 2m; c_1 + d_1 = 2n}} t^{2(m+n)} \binom{2m}{m} \binom{2n}{n} \frac{1}{a_1! b_1! c_1! d_1!} \left(\frac{1}{2\pi\sqrt{-1}} \int_{S^1} x^{a_1 - c_1 - b_1 + d_1} \frac{dx}{x} \right) \\
&= [\mathbf{B}(t(x + x^{-1}))\mathbf{B}(t(x^{-1} + x))]_{x^0}.
\end{aligned}$$

Using the definition of the twisted Bessel function, the Vandermonde identity and some elementary manipulations, we obtain

$$\begin{aligned}
(111) \quad & [\mathbf{B}(t(x + x^{-1}))^2]_{x^0} = \sum_{n \geq 0} \left(\sum_{a+b=n} \frac{1}{a!^2 b!^2} \right) [(x + x^{-1})^{2n}]_{x^0} t^{2n} \\
&= \sum_{n \geq 0} \left(\sum_{a=0}^n \frac{n!^2}{a!^2 (n-a)!^2} \right) \binom{2n}{n} \frac{t^{2n}}{n!^2} \\
&= \sum_{n \geq 0} \binom{2n}{n}^2 \frac{t^{2n}}{n!^2} \\
&= \sum_{n \geq 0} \frac{(2n!)^2}{n!^6} t^{2n}.
\end{aligned}$$

□

Applying the machinery. For $g \geq 3$ we can describe an inductive procedure. Denote the product of Bessel functions $\mathbf{B}(t(x + y))\mathbf{B}(t(x^{-1} + y^{-1}))$ by $\mathbf{T}_1(x, y)$. Observe that

$$\begin{aligned}
(112) \quad & \mathbf{T}_1(x, y^{-1}) = \mathbf{T}_1(x^{-1}, y) = \mathbf{B}(t(x + y^{-1}))\mathbf{B}(t(x^{-1} + y)) \\
& \mathbf{T}_1(x^{-1}, y^{-1}) = \mathbf{T}_1(x, y) = \mathbf{B}(t(x + y))\mathbf{B}(t(x^{-1} + y^{-1})).
\end{aligned}$$

This calculates the effect of changing the orientation of the boundary of the two-holed torus.

Definition 4.11. Define inductively using convolution the function

$$(113) \quad \mathbf{T}_{k+1}(x, y) := [\mathbf{T}_k(x, z)\mathbf{T}_1(z, y)]_{z^0}$$

The following proposition is an application of the usual machinery of determining the partition function by cutting a closed surface to easier pieces, and it explains the definition of $\mathbf{T}_{k+1}(x, y)$.

Proposition 4.12. *Let $\Sigma_{g,2}$ be a genus g surface with two holes, one oriented anticlockwise and the other oriented clockwise. Then the partition function of $\Sigma_{g,2}$ is given by $Z^{\text{EP}}(t)(\Sigma_{g,2}) = \mathbf{T}_g(x, y^{-1})$.*

Proof. Consider the necklace graph $\gamma_{1,2}$ as in Lemma 4.8 show in Figure 11(a). The genus two surface with two holes $\Sigma_{2,2}$ with one hole oriented anti-clockwise and the other hole oriented clockwise can be obtained gluing two $\Sigma_{1,2}$ as shown in Figure 15(a).

In terms of the dual graph this is obtained by gluing two open necklace graphs Figure 12 as shown in Figure 15(b).

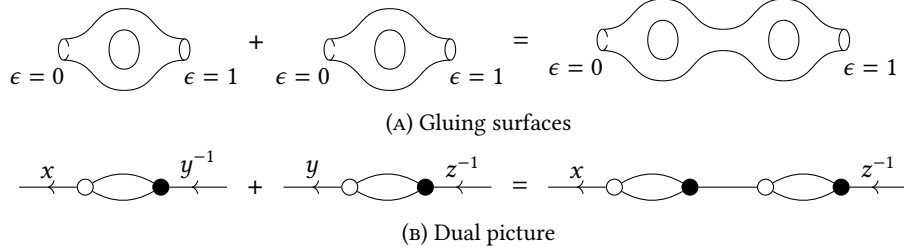


FIGURE 15. Two-holed surfaces of genus two by gluing

Then the partition function is given by

$$\begin{aligned}
 Z^{\text{sp}}(t)(\Sigma_{2,2}) &= \langle T_1(x, z^{-1}), T_1(z, y^{-1}) \rangle_z \\
 (114) \quad &= \frac{1}{2\pi\sqrt{-1}} \int_{S^1} T_1(x, z^{-1}) T_1(z^{-1}, y^{-1}) \frac{dz}{z} \\
 &= T_2(x, y^{-1}).
 \end{aligned}$$

Hence by repeating this process, gluing copies of $\gamma_{1,2}$ to increase the genus, and applying the TQFT formalism given by Proposition 3.5 we obtained the required result. \square

We now describe this result in terms of the period of graph potentials that we are interested in computing.

Proposition 4.13. *Let $(\gamma_{g,2}, \epsilon)$ be the (colored) dual graph of a surface with two holes obtained by gluing g copies of $\Sigma_{1,2}$ in a row. Then*

$$(115) \quad \mathcal{K}_{\gamma_{g,2},\epsilon}(t) = T_g(x, y^{(-1)^g}) = T_g(x, y^{(-1)^\epsilon}).$$

Proof. First of all observe that ϵ has the same parity as the genus g of the surface by construction.

Furthermore, if g is odd, then we need to make even number of cuts to get a disjoint union of $\Sigma_{1,2}$'s. Hence by Proposition 4.5, we get that $\mathcal{K}_{\gamma_{g,2},\epsilon}(t) = Z^{\text{sp}}(t)(\Sigma_{g,2})$. Then we are done by Proposition 4.12 when g is odd.

Now if g is even, then consider the graph $\gamma_{g-1,2}$ and an open necklace graph. Now by Proposition 4.4, we get

$$\begin{aligned}
 (116) \quad \mathcal{K}_{\gamma_{g,2},0}(t) &= [\mathcal{K}_{\gamma_{g-1,2},1}(t), T_1(z, y^{-1})]_{z^0} \\
 &= [T_{g-1}(x, z^{-1}), T_1(z^{-1}, y)]_{z^0} \\
 &= T_g(x, y).
 \end{aligned}$$

\square

A direct very useful corollary of the above proposition that removes the restriction on the matching of the parity of coloring and genus in Proposition 4.5 is the following

Corollary 4.14. *Let $\gamma_{g,2}$ be the open necklace graph of genus g with two half-edges as shown in Figure 11(b). Let c be a coloring of $\gamma_{g,2}$ and ϵ be the parity of the coloring, then*

$$(117) \quad \mathcal{K}_{\gamma_{g,2},c}(t) = T_g \left(x, y^{(-1)^\epsilon} \right).$$

Proof. If the parity of c matches up with the parity of the genus as in Proposition 4.5, then we are done. Otherwise choose one of the two half-edges and reverse the orientation of that half-edge. In the definition of $\mathcal{K}_{\gamma_{g,2},c}(t)$, we never integrate over a half-edge variable of the original graph γ , hence we are now reduced to the situation in Proposition 4.5. \square

Now we can use Proposition 4.13 to get a formula for the periods of the *closed* (i.e. without half-edges) genus g trivalent colored graphs (γ, c) .

Proposition 4.15. *Let γ be a trivalent graph of genus $g \geq 2$ without leaves and c a coloring of the vertices. Let $\epsilon \in \mathbb{F}_2$ denote the parity of the coloring. Then*

$$(118) \quad \mathcal{K}_{\gamma,c}(t) = \left[T_{g-1} \left(x, x^{(-1)^\epsilon} \right) \right]_{x^0}.$$

Proof. By Corollary 2.9 we know that $\mathcal{K}_{\gamma,c}(t)$ only depends on the parity of the coloring. Hence we can assume that the graph has either one or zero colored vertices. Moreover since the periods are invariants under mutations, we can assume that γ is the closed necklace graph of genus g as in Figure 16 with one or zero colored vertex.

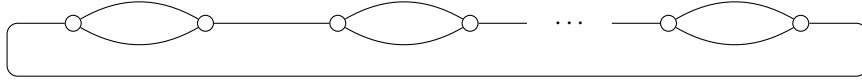


FIGURE 16. Closed necklace graph with many beads

First consider the case when g and c have the same parity. Then the result directly follows from Proposition 4.13 by applying Proposition 4.4. Now in the case g and c have opposite parity, then to compute $\mathcal{K}_{(\gamma_{g,0},\epsilon)}(t)$, cut an edge e of the graph γ to get the graph $(\gamma_{g-1,2}, \epsilon)$ considered in Proposition 4.13. Then by we are done by first applying Corollary 4.14 and then Proposition 4.4. \square

The main result. This proposition gives an effective method to compute the period of a graph potential, giving the main result of this section. It allows us to express (the inverse Fourier–Laplace transform of) the periods of the Laurent polynomials from Section 2 using trace-class operators in $\ell^2(\mathbb{Z})$.

Define

- A to be the Hilbert–Schmidt operator given by $T_1(x, y)$;
- S to be the bounded linear operator $S \left(\sum_{n \in \mathbb{Z}} a_n x^n \right) = \sum_{n \in \mathbb{Z}} a_n x^{-n}$.

We consider A as matrix with respect to the orthonormal basis and reinterpret Corollary 4.10 as follows.

Lemma 4.16. *Let $(\gamma_2, 1)$ be a genus two graph with one colored vertex, then*

$$(119) \quad \mathcal{K}_{\gamma_2, 1}(t) = \text{tr}(AS) = \sum_{n \geq 0} \frac{(2n!)^2}{n!^6} t^{2n}.$$

In particular the composition AS is trace class.

Since trace-class operators form an ideal, it follows that $A^{a+1}S^b$ is also trace-class for non-negative integers a, b . Moreover S commutes with A .

The following is the important computational tool for computing periods of graph potentials.

Theorem 4.17. *Let (γ, c) be a colored trivalent graph of genus $g \geq 2$ (without half-edges). Then,*

$$(120) \quad \tilde{\pi}_{\overline{W}_{\gamma, c}}(t) = \text{tr}(A^{g-1}S^{\epsilon+g})$$

where ϵ denotes the parity of the number of colored vertices in γ .

Proof. By Corollary 2.9 we can assume that the number of colored vertices is either zero or one. To show the equality in (120) we use Lemma 4.3 and Proposition 4.15, so that we need to show that

$$(121) \quad [\text{T}_{g-1}(x, x^{(-1)^\epsilon})]_{x^0} = \text{tr}(A^{g-1}S^{\epsilon+g}).$$

We do this by induction. If $g = 2$, then this follows from Corollary 4.10 for $\epsilon = 1$, whilst the case of $\epsilon = 0$ is analogous.

Next, observe that by the symmetry properties of A , we have that S commutes with A .

Now if g is arbitrary, we consider $\text{T}_{g-1}(x, y) \in \ell^2(\mathbb{Z})^{\otimes 2}$, writing it as $\sum_{i, j \in \mathbb{Z}} b_{i, j} x^i y^j$ for some matrix $B = (b_{i, j})$ in the orthonormal basis $\{x^i\}_{i \in \mathbb{Z}}$. We claim that $B = A^{g-1}S^{g-1}$. This follows by induction, using that S commutes with A .

Hence we get

$$(122) \quad \begin{aligned} [\text{T}_{g-1}(x, x^{(-1)^\epsilon})]_{x^0} &= \sum_{\substack{i, j \in \mathbb{Z} \\ i + (-1)^\epsilon j = 0}} b_{i, j} \\ &= \sum_{\substack{i, j \in \mathbb{Z} \\ i = (-1)^{\epsilon+1} j}} b_{i, j} \\ &= \sum_{i \in \mathbb{Z}} (S^{\epsilon+1} A^{g-1} S^{g-1})_{i, i} \\ &= \text{tr}(A^{g-1} S^{\epsilon+g}), \end{aligned}$$

again using that S commutes with A . □

Remark 4.18. This gives an explicit and efficient method to compute the period sequences, by truncating the power series in t . This method is independent of g , and the number of periods that one can compute depends only on the degree of the truncation, and *not* on g . As an illustration of this procedure, we have collected some output in Tables 1 and 2. In [10, Appendix B] we will discuss some patterns in this table.

Alternatively, using the main result of [10] one can compute quantum periods of these moduli spaces via the abelian/non-abelian correspondence in Gromov–Witten theory. But in this approach one fixes g and does a special analysis for each value of g (which is only feasible for low g). Developing the details of the abelian/non-abelian correspondence in this case and comparing the two methods is left for future work.

Some connections to other works in the literature. There exists a degeneration of our setup, which links it to mirror symmetry for Grassmannians of planes. For this we let γ be a genus zero graph with $n \geq 3$ half-edges and all vertices uncolored. The cardinality of the set of edges E is $2n - 3$ and we assign variables x_1, \dots, x_{2n-3} as before to all the half-edges. Consider the substitution

$$(123) \quad (x, y, z) \rightarrow \left(\frac{\tau}{X}, \frac{Y}{\tau}, \frac{Z}{\tau} \right).$$

where x, y, z are variables assigned to adjacent edges on a vertex v ; the X, Y, Z are new variables and τ is a formal parameter. In this set-up

$$(124) \quad \begin{aligned} \widetilde{W}_{v,0}(x, y, z) &= xyz + \frac{x}{yz} + \frac{y}{xz} + \frac{z}{xy} \\ &= \tau^{-1} \left(\frac{YZ}{X} + \tau^4 \frac{1}{XYZ} + \frac{XY}{Z} + \frac{ZX}{Y} \right) \end{aligned}$$

Now consider the Laurent polynomial $\widetilde{W}_{\gamma,0} = \sum_{v \in V} \widetilde{W}_{v,0}(x, y, z)$, and take $\lim_{\tau \rightarrow 0} \tau \widetilde{W}_{\gamma}$. This is a Laurent polynomial \mathcal{G}_{γ} in the variables X_1, \dots, X_{2n-3} . This is exactly the Laurent polynomial considered by Nohara–Ueda in [39, Theorem 1.6], and brings us to the following remark.

Remark 4.19. The above observation and the TQFT results from Theorem B and Proposition 3.5 tell us that the potential functions from Nohara and Ueda [39] associated to the Grassmannian of planes in an n -dimensional vector space also give a TQFT which one can call the *Grassmannian TQFT*. To the best of our knowledge this was not observed before.

In particular, by the above discussion and (124) the graph potential TQFT coming from moduli of bundles that we develop recovers the Grassmannian TQFT as a limit. This should be compared with a corresponding fact that genus zero conformal blocks recover invariants of tensor product representations in the limit.

g	p_0	p_2	p_4	p_6	p_8	p_{10}	p_{12}	p_{14}	p_{16}
2	1	8	216	8000	343000	16003008	788889024	40424237568	2131746903000
3	1	0	384	23040	3265920	435456000	68263641600	11300889600000	1984905402480000
4	1	0	576	11520	8769600	1175731200	445839609600	115772770713600	41211916193448000
5	1	0	768	0	16853760	928972800	1378578432000	295708763750400	237075779068128000
6	1	0	960	0	27518400	232243200	3112327680000	299893321728000	795162277629720000
7	1	0	1152	0	40763520	0	5892216422400	133905855283200	2006716647119184000
8	1	0	1344	0	56589120	0	9963493478400	22317642547200	4248683870158728000
9	1	0	1536	0	74995200	0	15571407667200	0	7983708676751808000
10	1	0	1728	0	95981760	0	22961207808000	0	13760135544283128000

TABLE 1. Period sequence for the odd graph potential

g	p_0	p_2	p_4	p_6	p_8	p_{10}	p_{12}	p_{14}	p_{16}	p_{18}
2	1	0	384	0	645120	0	1513881600	0	4132896768000	0
3	1	0	576	0	6350400	0	136604160000	0	3976941969000000	0
4	1	0	576	0	12640320	0	805929062400	0	80306439693480000	0
5	1	0	768	0	18144000	0	1915060224000	0	401643111149280000	0
6	1	0	960	0	27518400	0	3418888704000	0	1062973988196120000	0
7	1	0	1152	0	40763520	0	5953528627200	0	2211592605702480000	0
8	1	0	1344	0	56589120	0	9963493478400	0	4323671149117320000	0
9	1	0	1536	0	74995200	0	15571407667200	0	7994421145174464000	0
10	1	0	1728	0	95981760	0	22961207808000	0	13760135544283128000	0

TABLE 2. Period sequence for the even graph potential

REFERENCES

- [1] Casim Abbas. *An introduction to compactness results in symplectic field theory*. Springer, Heidelberg, 2014, pp. viii+252. ISBN: 978-3-642-31543-5.
- [2] Lowell Abrams. “Two-dimensional topological quantum field theories and Frobenius algebras.” In: *J. Knot Theory Ramifications* 5.5 (1996), pp. 569–587.
- [3] Mohammad Akhtar, Tom Coates, Sergey Galkin, and Alexander M. Kasprzyk. “Minkowski polynomials and mutations.” In: *SIGMA Symmetry Integrability Geom. Methods Appl.* 8 (94 2012), with an appendix (690 pages), 17 pages. arXiv: [1212.1785v1](#).
- [4] Michael Atiyah. “New invariants of 3- and 4-dimensional manifolds.” In: *The mathematical heritage of Hermann Weyl (Durham, NC, 1987)*. Vol. 48. Proc. Sympos. Pure Math. Amer. Math. Soc., Providence, RI, 1988, pp. 285–299.
- [5] Michael Atiyah. “Topological quantum field theories.” In: *Inst. Hautes Études Sci. Publ. Math.* 68 (1988), 175–186 (1989).
- [6] Dave Bayer and David Eisenbud. “Graph curves.” In: *Adv. Math.* 86.1 (1991). With an appendix by Sung Won Park, pp. 1–40.
- [7] Alexander A. Belavin, Alexander M. Polyakov, and Alexander B. Zamolodchikov. “Infinite conformal symmetry in two-dimensional quantum field theory.” In: *Nuclear Phys. B* 241.2 (1984), pp. 333–380.
- [8] Pieter Belmans, Sergey Galkin, and Swarnava Mukhopadhyay. *A combinatorial non-abelian Torelli theorem and random walks*. arXiv: [22???.????? \[math.AG\]](#).
- [9] Pieter Belmans, Sergey Galkin, and Swarnava Mukhopadhyay. *Decompositions of moduli spaces of vector bundles and graph potentials*. arXiv: [2009.05568v3 \[math.AG\]](#).
- [10] Pieter Belmans, Sergey Galkin, and Swarnava Mukhopadhyay. *Graph potentials and symplectic geometry of moduli spaces of vector bundles*. arXiv: [22???.????? \[math.SG\]](#).
- [11] Frédéric Bourgeois, Yakov Eliashberg, Helmut Hofer, Krzysztof Wysocki, and Eduard Zehnder. “Compactness results in symplectic field theory.” In: *Geom. Topol.* 7 (2003), pp. 799–888. arXiv: [math/0308183v3](#).
- [12] Tom Coates, Alessio Corti, Sergey Galkin, and Alexander Kasprzyk. “Quantum periods for 3-dimensional Fano manifolds.” In: *Geom. Topol.* 20.1 (2016), pp. 103–256. arXiv: [1303.3288v3](#).
- [13] Aliakbar Daemi and Kenji Fukaya. “Atiyah-Floer conjecture: a formulation, a strategy of proof and generalizations.” In: *Modern geometry: a celebration of the work of Simon Donaldson*. Vol. 99. Proc. Sympos. Pure Math. Amer. Math. Soc., Providence, RI, 2018, pp. 23–57.
- [14] Christopher Deninger. “Deligne periods of mixed motives, K -theory and the entropy of certain \mathbb{Z}^n -actions.” In: *J. Amer. Math. Soc.* 10.2 (1997), pp. 259–281.
- [15] Christopher Deninger and Klaus Schmidt. “Expansive algebraic actions of discrete residually finite amenable groups and their entropy.” In: *Ergodic Theory Dynam. Systems* 27.3 (2007), pp. 769–786. arXiv: [math/0605723v2](#).
- [16] Robertus Dijkgraaf. “A geometrical approach to two-dimensional Conformal Field Theory.” doctoralthesis. Utrecht University, 1989. URL: <https://dspace.library.uu.nl/handle/1874/210872>.
- [17] Yakov Eliashberg, Alexander Givental, and Helmut Hofer. “Introduction to symplectic field theory.” In: Special Volume, Part II. GAFA 2000 (Tel Aviv, 1999). Oct. 2000, pp. 560–673. arXiv: [math/0010059v1](#).
- [18] Andreas Floer. “An instanton-invariant for 3-manifolds.” In: *Comm. Math. Phys.* 118.2 (1988), pp. 215–240.
- [19] Andreas Floer. “Morse theory for Lagrangian intersections.” In: *J. Differential Geom.* 28.3 (1988), pp. 513–547.
- [20] William Fulton and Rahul Pandharipande. “Notes on stable maps and quantum cohomology.” In: *Algebraic geometry—Santa Cruz 1995*. Vol. 62. Proc. Sympos. Pure Math. Amer. Math. Soc., Providence, RI, 1997, pp. 45–96. arXiv: [alg-geom/9608011v2](#).

- [21] Israel Gelfand, Mikhail M. Kapranov, and Andrei Zelevinsky. *Discriminants, resultants and multidimensional determinants*. Modern Birkhäuser Classics. Reprint of the 1994 edition. Birkhäuser Boston, Inc., Boston, MA, 2008, pp. x+523. ISBN: 978-0-8176-4770-4.
- [22] Ángel González-Prieto, Marina Logares, and Vicente Muñoz. “A lax monoidal topological quantum field theory for representation varieties.” In: *Bull. Sci. Math.* 161 (2020), pp. 102871, 34. arXiv: [1709.05724v2](https://arxiv.org/abs/1709.05724v2).
- [23] Allen Hatcher and Willian Thurston. “A presentation for the mapping class group of a closed orientable surface.” In: *Topology* 19.3 (1980), pp. 221–237.
- [24] Ludmil Katzarkov. “Homological mirror symmetry and algebraic cycles.” In: *Homological mirror symmetry*. Vol. 757. Lecture Notes in Phys. Springer, Berlin, 2009, pp. 125–152.
- [25] Ludmil Katzarkov, Maxim Kontsevich, and Tony Pantev. “Bogomolov-Tian-Todorov theorems for Landau-Ginzburg models.” In: *J. Differential Geom.* 105.1 (2017), pp. 55–117. arXiv: [1409.5996v2](https://arxiv.org/abs/1409.5996v2).
- [26] Maxim Kontsevich. “Homological algebra of mirror symmetry.” In: *Proceedings of the International Congress of Mathematicians, Vol. 1, 2 (Zürich, 1994)*. Birkhäuser, Basel, 1995, pp. 120–139. arXiv: [alg-geom/9411018v1](https://arxiv.org/abs/alg-geom/9411018v1).
- [27] Maxim Kontsevich. “Lectures at ENS Paris.” <http://math.uchicago.edu/~drinfeld/langlands/kontsevich.ps>. 1998.
- [28] Maxim Kontsevich and Yuri I. Manin. “Gromov-Witten classes, quantum cohomology, and enumerative geometry.” In: *Comm. Math. Phys.* 164.3 (1994), pp. 525–562. arXiv: [hep-th/9402147v2](https://arxiv.org/abs/hep-th/9402147v2).
- [29] Jacob Lurie. “On the classification of topological field theories.” In: *Current developments in mathematics, 2008*. Int. Press, Somerville, MA, 2009, pp. 129–280. arXiv: [0905.0465v1](https://arxiv.org/abs/0905.0465v1).
- [30] Travis Mandel and Helge Ruddat. “Descendant log Gromov-Witten invariants for toric varieties and tropical curves.” In: *Trans. Amer. Math. Soc.* 373.2 (2020), pp. 1109–1152. arXiv: [1612.02402](https://arxiv.org/abs/1612.02402).
- [31] Travis Mandel and Helge Ruddat. *Tropical quantum field theory, mirror polyvector fields, and multiplicities of tropical curves*. 2019. arXiv: [1902.07183v1](https://arxiv.org/abs/1902.07183v1).
- [32] Hannah Markwig and Johannes Rau. “Tropical descendant Gromov-Witten invariants.” In: *manuscripta math.* 129.3 (2009), pp. 293–335. arXiv: [0809.1102](https://arxiv.org/abs/0809.1102).
- [33] Grigory Mikhalkin. “Enumerative tropical algebraic geometry in \mathbb{R}^2 .” In: *J. Amer. Math. Soc.* 18.2 (2005), pp. 313–377. arXiv: [math/0312530](https://arxiv.org/abs/math/0312530).
- [34] Grigory Mikhalkin. “Moduli spaces of rational tropical curves.” In: *Proceedings of Gökova Geometry-Topology Conference 2006*. Gökova Geometry/Topology Conference (GGT), Gökova, 2007, pp. 39–51. arxiv: [0704.0839](https://arxiv.org/abs/0704.0839).
- [35] Vicente Muñoz. “Quantum cohomology of the moduli space of stable bundles over a Riemann surface.” In: *Duke Math. J.* 98.3 (1999), pp. 525–540. arXiv: [alg-geom/9711030v1](https://arxiv.org/abs/alg-geom/9711030v1).
- [36] Vicente Muñoz. “Ring structure of the Floer cohomology of $\Sigma \times S^1$.” In: *Topology* 38.3 (1999), pp. 517–528. arXiv: [dg-ga/9710029v1](https://arxiv.org/abs/dg-ga/9710029v1).
- [37] M. S. Narasimhan and S. Ramanan. “Moduli of vector bundles on a compact Riemann surface.” In: *Ann. of Math. (2)* 89 (1969), pp. 14–51.
- [38] Peter Newstead. “Stable bundles of rank 2 and odd degree over a curve of genus 2.” In: *Topology* 7 (1968), pp. 205–215.
- [39] Yuichi Nohara and Kazushi Ueda. “Toric degenerations of integrable systems on Grassmannians and polygon spaces.” In: *Nagoya Math. J.* 214 (2014), pp. 125–168. arXiv: [1111.4809v2](https://arxiv.org/abs/1111.4809v2).
- [40] Sebastian Novak and Ingo Runkel. “State sum construction of two-dimensional topological quantum field theories on spin surfaces.” In: *J. Knot Theory Ramifications* 24.5 (2015), pp. 1550028, 84. arXiv: [1402.2839v2](https://arxiv.org/abs/1402.2839v2).
- [41] *PARI/GP version 2.14.0*. available from <http://pari.math.u-bordeaux.fr/>. The PARI Group. 2020. URL: <http://pari.math.u-bordeaux.fr>.
- [42] Akihiro Tsuchiya, Kenji Ueno, and Yasuhiko Yamada. “Conformal field theory on universal family of stable curves with gauge symmetries.” In: *Integrable systems in quantum field theory*

- and statistical mechanics*. Vol. 19. Adv. Stud. Pure Math. Academic Press, Boston, MA, 1989, pp. 459–566.
- [43] Erik Verlinde. “Fusion rules and modular transformations in 2D conformal field theory.” In: *Nuclear Phys. B* 300.3 (1988), pp. 360–376.

DEPARTMENT OF MATHEMATICS, UNIVERSITÉ DE LUXEMBOURG, 6, AVENUE DE LA FONTE, L-4364 ESCH-SUR-ALZETTE, LUXEMBOURG

PUC-RIO, DEPARTAMENTO DE MATEMÁTICA, RUA MARQUÊS DE SÃO VICENTE 225, GÁVEA, RIO DE JANEIRO, (ON LEAVE FROM HSE UNIVERSITY, RUSSIAN FEDERATION)

SCHOOL OF MATHEMATICS, TATA INSTITUTE OF FUNDAMENTAL RESEARCH, 1 HOMI BHABHA ROAD, NAVY NAGAR, COLABA, MUMBAI 400005

Email address: pieter.belmans@uni.lu, arxiv-tqft@galkin.org.ru, swarnava@math.tifr.res.in